Multi-parametric Solution-path Algorithm for Instance-weighted Support Vector Machines

Masayuki Karasuyama   KRSYM@GOAT.ICS.NITECH.AC.JP
Naoyuki Harada   HARADA@GOAT.ICS.NITECH.AC.JP
Department of Engineering
Nagoya Institute of Technology
Nagoya, Aichi 466-8555, Japan

Masashi Sugiyama   SUGI@CS.TITECH.AC.JP
Department of Computer Science
Tokyo Institute of Technology
Tokyo 152-8552 Japan

Ichiro Takeuchi   TAKEUCHI.ICHIRO@NITECH.AC.JP
Department of Engineering
Nagoya Institute of Technology
Nagoya, Aichi 466-8555, Japan

Editor:

Abstract

An *instance-weighted* variant of the support vector machine (SVM) has attracted considerable attention recently since they are useful in various machine learning tasks such as non-stationary data analysis, heteroscedastic data modeling, transfer learning, learning to rank, and transduction. An important challenge in these scenarios is to overcome the computational bottleneck—instance weights often change dynamically or adaptively, and thus the weighted SVM solutions must be repeatedly computed. In this paper, we develop an algorithm that can efficiently and exactly update the weighted SVM solutions for arbitrary change of instance weights. Technically, this contribution can be regarded as an extension of the conventional *solution-path* algorithm for a single regularization parameter to multiple instance-weight parameters. However, this extension gives rise to a significant problem that *breakpoints* (at which the solution path turns) have to be identified in high-dimensional space. To facilitate this, we introduce a parametric representation of instance weights. We also provide a geometric interpretation in weight space using a notion of *critical region*: a polyhedron in which the current affine solution remains to be optimal. Then we find breakpoints at intersections of the solution path and boundaries of polyhedrons. Through extensive experiments on various practical applications, we demonstrate the usefulness of the proposed algorithm.

Keywords: Parametric programming, solution path, weighted support vector machines.

1. Introduction

The most fundamental principle of machine learning would be the *empirical risk minimization*, i.e., the sum of empirical losses over training instances is minimized:

$$\min \sum_i L_i,$$

where L_i denotes the empirical loss for the i-th training instance. This empirical risk minimization approach was proved to produce *consistent* estimators (Vapnik, 1995). On the other hand, one may also consider an *instance-weighted* variant of empirical risk minimization:

$$\min \sum_i C_i L_i,$$

where C_i denotes the weight for the i-th training instance. This weighted variant plays an important role in various machine learning tasks:

- **Non-stationary data analysis:** When training instances are provided in a sequential manner under changing environment, smaller weights are often assigned to older instances for imposing some 'forgetting' effect (Murata et al., 2002; Cao and Tay, 2003).

- **Heteroscedastic data modeling:** A supervised learning setup where the noise level in output values depends on input points is said to be *heteroscedastic*. In heteroscedastic data modeling, larger weights are often assigned to instances with smaller noise variance (Kersting et al., 2007). The traditional *Gauss-Markov theorem* (Albert, 1972) forms the basis of this idea.

- **Covariate shift adaptation, transfer learning, and multi-task learning:** A supervised learning situation where training and test *inputs* follow different distributions is called covariate shift. Under covariate shift, using the *importance* (the ratio of the test and training input densities) as instance weights assures the consistency of estimators (Shimodaira, 2000). Similar importance-weighting ideas can be applied also to transfer learning (where data in one domain is transferred to another domain) (Jiang and Zhai, 2007) and multi-task learning (where multiple learning problems are solved simultaneously by sharing training instances) (Bickel et al., 2008).

- **Learning to rank and ordinal regression:** The goal of ranking (a.k.a. ordinal regression) is to give an ordered list of items based on their relevance (Herbrich et al., 2000; Liu, 2009). In practical ranking tasks such as information retrieval, users are often not interested in the entire ranking list, but only in the top few items. In order to improve the prediction accuracy in the top of the list, larger weights are often assigned to higher-ranked items (Xu et al., 2006).

- **Transduction and semi-supervised learning:** Transduction is a supervised learning setup where the goal is not to learn the entire input-output mapping, but only to estimate the output values for pre-specified unlabeled input points (Vapnik, 1995). A

2

popular approach to transduction is to label the unlabeled samples using the current estimator, and then modify the estimator using the 'self-labeled' samples (Joachims, 1999; Raina et al., 2007). In this procedure, smaller weights are usually assigned to the self-labeled samples than the originally-labeled samples due to their high uncertainty.

A common challenge in the research of instance-weighted learning has been to overcome the computational issue. In many of these tasks, instance weights often change dynamically or adaptively, and thus the instance-weighted solutions must be repeatedly computed. For example, in on-line learning, every time when a new instance is observed, all the instance weights must be updated in such a way that newer instances have larger weights and older instances have smaller weights. Model selection in instance-weighted learning also poses a considerable computational burden. In many of the above scenarios, we only have qualitative knowledge about instance weights. For example, in the aforementioned ranking problem, we only know that higher-ranked items should have larger weights than lower-ranked items, but it is often difficult to know how large or small these weights should be. The problem of selecting the optimal weighting patterns is an instance of model selection, and many instance-weighted solutions with various weighting patterns must be computed in the model selection phase. The goal of this paper is to alleviate the computational bottleneck of instance-weighted learning.

In this paper, we focus on the *support vector machine* (SVM) (Boser et al., 1992; Cortes and Vapnik, 1995), which is a popular classification algorithm minimizing a regularized empirical risk:

$$\min R + C \sum_i L_i,$$

where R is a regularization term and $C \geq 0$ controls the trade-off between the regularization effect and the empirical risk minimization. We consider an instance-weighted variant of SVM, which we refer to as the *weighted SVM* (WSVM) (Lin et al., 2002; Lin and Wang, 2002; Yang et al., 2007):

$$\min R + \sum_i C_i L_i.$$

For ordinary SVM, the *solution path algorithm* was proposed (Hastie et al., 2004), which allows efficient computation of SVM solutions for all C by utilizing the piecewise-linear structure of the solutions w.r.t. C. This technique is known as *parametric programming* in the optimization community (Best, 1982; Ritter, 1984; Allgower and Georg, 1993; Bennett and Bredensteiner, 1997), and has been applied to various machine learning tasks recently (Fine and Scheinberg, 2002; Zhu et al., 2004; Bach et al., 2006; Gunter and Zhu, 2007; Rosset and Zhu, 2007; Lee and Scott, 2007; Sjostrand et al., 2007; Wang et al., 2008; Arreola et al., 2008; Takeuchi et al., 2009; Kanamori et al., 2009); the *incremental-decremental SVM algorithm*, which efficiently follows the piecewise-linear solution path when some training instances are added or removed from the training set, is also based on the same parametric programming technique (Cauwenberghs and Poggio, 2001; Laskov et al., 2006; Karasuyama and Takeuchi, 2009).

3

The solution path algorithms described above have been developed for problems with a *single* hyper-parameter. Recently, attention has been paid to studying solution-path tracking in two-dimensional hyper-parameter space. For example, Wang et al. (2008) developed a path-following algorithm for regularization parameter C and an insensitive zone thickness ε in *support vector regression* (Vapnik et al., 1996; Mattera and Haykin, 1999; Müller et al., 1999). Rosset (2009) studied a path-following algorithm for regularization parameter λ and quantile parameter τ in *kernel quantile regression* (Takeuchi et al., 2006). However, these works are highly specialized to specific problem structure of bivariate path-following, and it is not straightforward to extend them to more than two hyper-parameters. Thus, the existing approaches may not be applicable to path-following of WSVM, which contains n-dimensional instance-weight parameters $\boldsymbol{c} = [C_1, \ldots, C_n]^{\top}$, where n is the number of training instances.

In order to go beyond the limitation of the existing approaches, we derive a general solution path algorithm for efficiently computing the solution path of *multiple* instance-weight parameters $\boldsymbol{c}$ in WSVM. This extension involves a significant problem that *breakpoints* (at which the solution path turns) have to be identified in high-dimensional space. To facilitate this, we introduce a parametric representation of instance weights. We also provide a geometric interpretation in weight space using a notion of *critical region* from the studies of *multi-parametric programming* (Gal and Nedoma, 1972; Pistikopoulos et al., 2007). A critical region is a polyhedron in which the current *affine* solution remains to be optimal (see Figure 2). This enables us to find breakpoints at intersections of the solution path and the boundaries of polyhedrons.

This paper is organized as follows. Section 2 reviews the definition of WSVM and its optimality conditions. Then we derive the path-following algorithm for WSVM in Section 3. Section 4 is devoted to experimentally illustrating advantages of our algorithm on a toy problem, on-line time-series analysis and covariate shift adaptation. Extensions to regression, ranking, and transduction scenarios are discussed in Section 5. Finally, we conclude in Section 6.

2. Problem Formulation

In this section, we review the definition of the *weighted support vector machine* (WSVM) and its optimality conditions. For the moment, we focus on binary classification scenarios. Later in Section 5, we extend our discussion to more general scenarios such as regression, ranking, and transduction.

2.1 WSVM

Let us consider a binary classification problem. Denote n training instances as $\{(\boldsymbol{x}_i, y_i)\}_{i=1}^{n}$, where $\boldsymbol{x}_i \in \mathcal{X} \subseteq \mathbb{R}^p$ is the input and $y_i \in \{-1, +1\}$ is the output label.

SVM (Boser et al., 1992; Cortes and Vapnik, 1995) is a learning algorithm of a linear decision boundary

$$f(\boldsymbol{x}) = \boldsymbol{w}^{\top} \Phi(\boldsymbol{x}) + b$$

in a feature space $\mathcal{F}$, where $\Phi : \mathcal{X} \rightarrow \mathcal{F}$ is a map from the input space $\mathcal{X}$ to the feature space $\mathcal{F}$, $\boldsymbol{w} \in \mathcal{F}$ is a coefficient vector, $b \in \mathbb{R}$ is a bias term, and $^{\top}$ denotes the transpose.

The parameters $\boldsymbol{w}$ and b are learned as

$$\min_{\boldsymbol{w},b} \frac{1}{2}\|\boldsymbol{w}\|_2^2 + C\sum_{i=1}^{n}[1 - y_i f(\boldsymbol{x}_i)]_+, \tag{1}$$

where $\frac{1}{2}\|\boldsymbol{w}\|_2^2$ is the regularization term, $\|\cdot\|$ denotes the Euclidean norm, C is the trade-off parameter, and

$$[z]_+ = \max\{0, z\}.$$

$[1 - y_i f(\boldsymbol{x}_i)]_+$ is the so-called *hinge-loss* for the i-th training instance.

WSVM is an extension of the ordinary SVM so that each training instance possesses its own weight (Lin et al., 2002; Lin and Wang, 2002; Yang et al., 2007):

$$\min_{\boldsymbol{w},b} \frac{1}{2}\|\boldsymbol{w}\|_2^2 + \sum_{i=1}^{n} C_i[1 - y_i f(\boldsymbol{x}_i)]_+, \tag{2}$$

where C_i is the weight for the i-th training instance. WSVM includes the ordinary SVM as a special case when $C_i = C$ for $i = 1, \ldots, n$. The primal optimization problem (2) is expressed as the following quadratic program:

$$\min_{\boldsymbol{w},b,\{\xi_i\}_{i=1}^n} \frac{1}{2}\|\boldsymbol{w}\|_2^2 + \sum_{i=1}^{n} C_i \xi_i, \tag{3}$$
$$\text{s.t. } y_i f(\boldsymbol{x}_i) \geq 1 - \xi_i, \ \xi_i \geq 0, \ i = 1, \ldots, n.$$

The goal of this paper is to derive an algorithm that can efficiently compute the sequence of WSVM solutions for arbitrary weighting patterns of $\boldsymbol{c} = [C_1, \ldots, C_n]^\top$.

2.2 Optimization in WSVM

Here we review basic optimization issues of WSVM which are used in the following section.

Introducing Lagrange multipliers $\alpha_i \geq 0$ and $\rho_i \geq 0$, we can write the *Lagrangian* of (3) as

$$L = \frac{1}{2}\|\boldsymbol{w}\|^2 + \sum_{i=1}^{n} C_i \xi_i - \sum_{i=1}^{n} \alpha_i \{y_i f(\boldsymbol{x}_i) - 1 + \xi_i\} - \sum_{i=1}^{n} \rho_i \xi_i. \tag{4}$$

Setting the derivatives of the above Lagrangian w.r.t. the primal variables $\boldsymbol{w}$, b, and ξ_i to zero, we obtain

$$\frac{\partial L}{\partial \boldsymbol{w}} = \boldsymbol{0} \ \Leftrightarrow \ \boldsymbol{w} = \sum_{i=1}^{n} \alpha_i y_i \Phi(\boldsymbol{x}_i),$$

$$\frac{\partial L}{\partial b} = 0 \ \Leftrightarrow \ \sum_{i=1}^{n} \alpha_i y_i = 0,$$

$$\frac{\partial L}{\partial \xi_i} = 0 \ \Leftrightarrow \ \alpha_i = C_i - \rho_i, \ i = 1, \ldots, n,$$

where $\mathbf{0}$ denotes the vector with all zeros. Substituting these equations into (4), we arrive at the following dual problem:

$$\max_{\{\alpha_i\}_{i=1}^n} \quad -\frac{1}{2}\sum_{i=1}^n\sum_{j=1}^n \alpha_i\alpha_j Q_{ij} + \sum_{i=1}^n \alpha_i$$

$$\text{s.t.} \quad \sum_{i=1}^n y_i\alpha_i = 0, \ 0 \le \alpha_i \le C_i, \tag{5}$$

where

$$Q_{ij} = y_i y_j K(\boldsymbol{x}_i, \boldsymbol{x}_j),$$

and $K(\boldsymbol{x}_i, \boldsymbol{x}_j) = \Phi(\boldsymbol{x}_i)^T \Phi(\boldsymbol{x}_j)$ is a *reproducing kernel* (Aronszajn, 1950). The discriminant function $f : \mathcal{X} \to \mathbb{R}$ is represented in the following form:

$$f(\boldsymbol{x}) = \sum_{i=1}^n \alpha_i y_i K(\boldsymbol{x}, \boldsymbol{x}_i) + b.$$

The optimality conditions of the dual problem (5), called the *Karush-Kuhn-Tucker (KKT) conditions* (Boyd and Vandenberghe, 2004), are summarized as follows:

$$y_i f(\boldsymbol{x}_i) \ge 1, \quad \text{if} \quad \alpha_i = 0, \tag{6a}$$
$$y_i f(\boldsymbol{x}_i) = 1, \quad \text{if} \quad 0 < \alpha_i < C_i, \tag{6b}$$
$$y_i f(\boldsymbol{x}_i) \le 1, \quad \text{if} \quad \alpha_i = C_i, \tag{6c}$$
$$\sum_{i=1}^n y_i\alpha_i = 0. \tag{6d}$$

We define the following three index sets for later use:

$$\mathcal{O} = \{i \mid \alpha_i = 0\}, \tag{7a}$$
$$\mathcal{M} = \{i \mid 0 < \alpha_i < C_i\}, \tag{7b}$$
$$\mathcal{I} = \{i \mid \alpha_i = C_i\}, \tag{7c}$$

where $\mathcal{O}$, $\mathcal{M}$, and $\mathcal{I}$ stand for 'Outside the margin' ($y_i f(\boldsymbol{x}_i) \ge 1$), 'on the Margin' ($y_i f(\boldsymbol{x}_i) = 1$), and 'Inside the margin' ($y_i f(\boldsymbol{x}_i) \le 1$), respectively (see Figure 1).

In what follows, the subscript by an index set such as $\boldsymbol{v}_{\mathcal{I}}$ for a vector $\boldsymbol{v} \in \mathbb{R}^n$ indicates a sub-vector of $\boldsymbol{v}$ whose elements are indexed by $\mathcal{I}$. For example, for $\boldsymbol{v} = (a, b, c)^\top$ and $\mathcal{I} = \{1, 3\}$, $\boldsymbol{v}_{\mathcal{I}} = (a, c)^\top$. Similarly, the subscript by two index sets such as $\boldsymbol{M}_{\mathcal{M},\mathcal{O}}$ for a matrix $\boldsymbol{M} \in \mathbb{R}^{n \times n}$ denotes a sub-matrix whose rows and columns are indexed by $\mathcal{M}$ and $\mathcal{O}$, respectively. The principal sub-matrix such as $\boldsymbol{M}_{\mathcal{M},\mathcal{M}}$ is abbreviated as $\boldsymbol{M}_{\mathcal{M}}$.

3. Solution-Path Algorithm for WSVM

The path-following algorithm for the ordinary SVM (Hastie et al., 2004) computes the entire solution path for the single regularization parameter C. In this section, we develop a path-following algorithm for the vector of weights $\boldsymbol{c} = [C_1, \dots, C_n]^\top$. Our proposed algorithm keeps track of the optimal α_i and b when the weight vector $\boldsymbol{c}$ is changed.
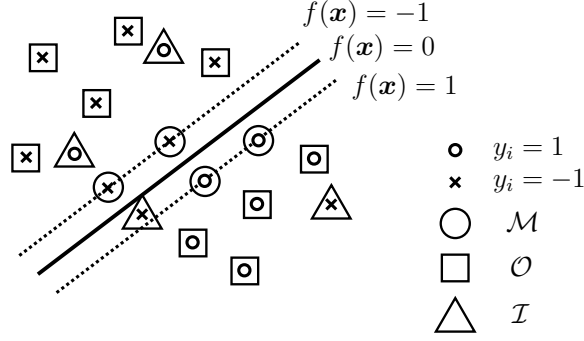
Figure 1: The partitioning of the data points in SVM.

3.1 Analytic Expression of WSVM Solutions

Let

$$\boldsymbol{\alpha} = \begin{bmatrix} \alpha_1 \\ \vdots \\ \alpha_n \end{bmatrix}, \ \boldsymbol{y} = \begin{bmatrix} y_1 \\ \vdots \\ y_n \end{bmatrix}, \ \text{and } \boldsymbol{Q} = \begin{bmatrix} Q_{11} & \cdots & Q_{1n} \\ \vdots & \ddots & \vdots \\ Q_{n1} & \cdots & Q_{nn} \end{bmatrix}.$$

Then, using the index sets (7b) and (7c), we can expand one of the KKT conditions, (6b), as

$$\boldsymbol{Q}_{\mathcal{M}}\boldsymbol{\alpha}_{\mathcal{M}} + \boldsymbol{Q}_{\mathcal{M},\mathcal{I}}\boldsymbol{c}_{\mathcal{I}} + \boldsymbol{y}_{\mathcal{M}}b = \mathbf{1}, \tag{8}$$

where $\mathbf{1}$ denotes the vector with all ones. Similarly, another KKT condition (6d) is expressed as

$$\boldsymbol{y}_{\mathcal{M}}^{\top}\boldsymbol{\alpha}_{\mathcal{M}} + \boldsymbol{y}_{\mathcal{I}}^{\top}\boldsymbol{c}_{\mathcal{I}} = 0. \tag{9}$$

Let

$$\boldsymbol{M} = \begin{bmatrix} 0 & \boldsymbol{y}_{\mathcal{M}}^{\top} \\ \boldsymbol{y}_{\mathcal{M}} & \boldsymbol{Q}_{\mathcal{M}} \end{bmatrix}.$$

Then (8) and (9) can be compactly expressed as the following system of $|\mathcal{M}| + 1$ linear equations, where $|\mathcal{M}|$ denotes the number of elements in the set $\mathcal{M}$:

$$\boldsymbol{M}\begin{bmatrix} b \\ \boldsymbol{\alpha}_{\mathcal{M}} \end{bmatrix} + \begin{bmatrix} \boldsymbol{y}_{\mathcal{I}}^{\top} \\ \boldsymbol{Q}_{\mathcal{M},\mathcal{I}} \end{bmatrix} \boldsymbol{c}_{\mathcal{I}} = \begin{bmatrix} 0 \\ \mathbf{1} \end{bmatrix}. \tag{10}$$

Solving (10) w.r.t. b and $\boldsymbol{\alpha}_{\mathcal{M}}$, we obtain

$$\begin{bmatrix} b \\ \boldsymbol{\alpha}_{\mathcal{M}} \end{bmatrix} = -\boldsymbol{M}^{-1}\begin{bmatrix} \boldsymbol{y}_{\mathcal{I}}^{\top} \\ \boldsymbol{Q}_{\mathcal{M},\mathcal{I}} \end{bmatrix} \boldsymbol{c}_{\mathcal{I}} + \boldsymbol{M}^{-1}\begin{bmatrix} 0 \\ \mathbf{1} \end{bmatrix}, \tag{11}$$

where we implicitly assumed that $\boldsymbol{M}$ is invertible[1]. Since b and $\boldsymbol{\alpha}_{\mathcal{M}}$ are *affine* w.r.t. $\boldsymbol{c}_{\mathcal{I}}$, we can calculate the change of b and $\boldsymbol{\alpha}_{\mathcal{M}}$ by (11) as long as the weight vector $\boldsymbol{c}$ is changed

---

1. The invertibility of the matrix $\boldsymbol{M}$ is assured if and only if the submatrix $\boldsymbol{Q}_{\mathcal{M}}$ is positive definite in the subspace $\{\boldsymbol{z} \in \mathbb{R}^{|\mathcal{M}|} \mid \boldsymbol{y}_{\mathcal{M}}^{\top}\boldsymbol{z} = 0\}$. We assume this technical condition here. A notable exceptional case is that $\mathcal{M}$ is empty—we will discuss how to cope with this case in detail in Section 3.3.

continuously. By the definition of $\mathcal{I}$ and $\mathcal{O}$, the remaining parameters $\boldsymbol{\alpha}_\mathcal{I}$ and $\boldsymbol{\alpha}_\mathcal{O}$ are merely given by

$$\boldsymbol{\alpha}_\mathcal{I} = \boldsymbol{c}_\mathcal{I}, \tag{12}$$

$$\boldsymbol{\alpha}_\mathcal{O} = \boldsymbol{0}. \tag{13}$$

A change of the index sets $\mathcal{M}$, $\mathcal{O}$, and $\mathcal{I}$ is called an *event*. As long as no event occurs, the WSVM solutions for all $\boldsymbol{c}$ can be computed by (11)–(13) since all the KKT conditions (6a)–(6d) are still satisfied. However, when an event occurs, we need to check the violation of the KKT conditions. Below, we address the issue of event detection when $\boldsymbol{c}$ is changed.

3.2 Event Detection

Suppose we want to change the weight vector from $\boldsymbol{c}^{(\mathrm{old})}$ to $\boldsymbol{c}^{(\mathrm{new})}$ (see Figure 2). This can be achieved by moving the weight vector $\boldsymbol{c}^{(\mathrm{old})}$ toward the direction of $\boldsymbol{c}^{(\mathrm{new})} - \boldsymbol{c}^{(\mathrm{old})}$.

Let us write the line segment between $\boldsymbol{c}^{(\mathrm{old})}$ and $\boldsymbol{c}^{(\mathrm{new})}$ in the following parametric form

$$\boldsymbol{c}(\theta) = \boldsymbol{c}^{(\mathrm{old})} + \theta \left(\boldsymbol{c}^{(\mathrm{new})} - \boldsymbol{c}^{(\mathrm{old})} \right), \ \theta \in [0, 1],$$

where θ is a parameter. This parametrization allows us to derive a path-following algorithm between arbitrary $\boldsymbol{c}^{(\mathrm{old})}$ and $\boldsymbol{c}^{(\mathrm{new})}$ by considering the change of the solutions when θ is moved from 0 to 1. Suppose we are currently at $\boldsymbol{c}(\theta)$ on the path, and the current solution is $(b, \boldsymbol{\alpha})$. Let

$$\boldsymbol{\Delta c} = \Delta\theta \left(\boldsymbol{c}^{(\mathrm{new})} - \boldsymbol{c}^{(\mathrm{old})} \right), \ \Delta\theta \geq 0, \tag{14}$$

where the operator Δ represents the amount of change of each variable from the current value. If $\Delta\theta$ is increased from 0, we may encounter a point at which some of the KKT conditions (6a)–(6c) do not hold. This can be checked by investigating the following conditions.

$$\begin{cases} y_i f(\boldsymbol{x}_i) + y_i \Delta f(\boldsymbol{x}_i) \geq 1, & i \in \mathcal{O}, \\ \alpha_i + \Delta\alpha_i > 0, & i \in \mathcal{M}, \\ \alpha_i + \Delta\alpha_i - (C_i + \Delta C_i,) < 0, & i \in \mathcal{M}, \\ y_i f(\boldsymbol{x}_i) + y_i \Delta f(\boldsymbol{x}_i) \leq 1, & i \in \mathcal{I}. \end{cases} \tag{15}$$

The set of inequalities (15) defines a convex polyhedron, called a *critical region* in the multi-parametric programming literature (Pistikopoulos et al., 2007). The event points lie on the border of critical regions, as illustrated in Figure 2.

We detect an event point by checking the conditions (15) along the solution path as follows. Using (11), we can express the changes of b and $\boldsymbol{\alpha}_\mathcal{M}$ as

$$\left[\begin{array}{c} \Delta b \\ \boldsymbol{\Delta\alpha}_\mathcal{M} \end{array} \right] = \Delta\theta\phi, \tag{16}$$

where

$$\phi = -\boldsymbol{M}^{-1} \left[\begin{array}{c} \boldsymbol{y}_\mathcal{I}^\top \\ \boldsymbol{Q}_{\mathcal{M},\mathcal{I}} \end{array} \right] (\boldsymbol{c}_\mathcal{I}^{(\mathrm{new})} - \boldsymbol{c}_\mathcal{I}^{(\mathrm{old})}). \tag{17}$$
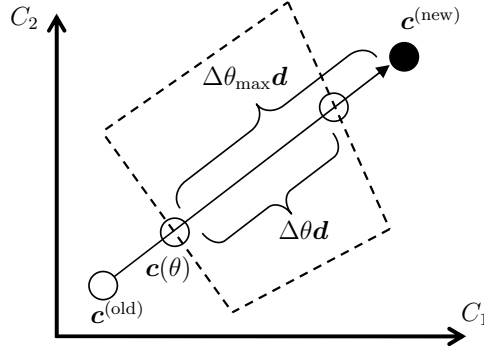
Figure 2: The schematic illustration of path-following in the space of $\boldsymbol{c} \in \mathbb{R}^2$, where the WSVM solution is updated from $\boldsymbol{c}^{(\text{old})}$ to $\boldsymbol{c}^{(\text{new})}$. Suppose we are currently at $\boldsymbol{c}(\theta)$. The vector $\boldsymbol{d}$ represents the update direction $\boldsymbol{c}^{(\text{new})} - \boldsymbol{c}^{(\text{old})}$, and the polygonal region enclosed by dashed lines indicates the current critical region. Although $\boldsymbol{c}(\theta) + \Delta\theta_{\max}\boldsymbol{d}$ seems to directly lead the solution to $\boldsymbol{c}^{(\text{new})}$, the maximum possible update from $\boldsymbol{c}(\theta)$ is $\Delta\theta\boldsymbol{d}$; otherwise the KKT conditions are violated. To go beyond the border of the critical region, we need to update the index sets $\mathcal{M}$, $\mathcal{I}$, and $\mathcal{O}$ to fulfill the KKT conditions.

Furthermore, $y_i \Delta f(\boldsymbol{x}_i)$ is expressed as

$$
y_i \Delta f(\boldsymbol{x}_i) = \begin{bmatrix} y_i & \boldsymbol{Q}_{i,\mathcal{M}} \end{bmatrix} \begin{bmatrix} \Delta b \\ \boldsymbol{\Delta\alpha}_{\mathcal{M}} \end{bmatrix} + \boldsymbol{Q}_{i,\mathcal{I}} \boldsymbol{\Delta c}_{\mathcal{I}}
$$
$$
= \Delta\theta \psi_i, \tag{18}
$$

where

$$
\psi_i = \begin{bmatrix} y_i & \boldsymbol{Q}_{i,\mathcal{M}} \end{bmatrix} \boldsymbol{\phi} + \boldsymbol{Q}_{i,\mathcal{I}}(\boldsymbol{c}_{\mathcal{I}}^{(\text{new})} - \boldsymbol{c}_{\mathcal{I}}^{(\text{old})}). \tag{19}
$$

Let us denote the elements of the index set $\mathcal{M}$ as

$$
\mathcal{M} = \{m_1, \ldots, m_{|\mathcal{M}|}\}.
$$

Substituting (16) and (18) into the inequalities (15), we can obtain the maximum step-length with no event occurrence as

$$
\Delta\theta = \min_{i \in \{1, \ldots, |\mathcal{M}|\}, j \in \mathcal{I} \cup \mathcal{O}} \left\{ -\frac{\alpha_{m_i}}{\phi_{i+1}}, \frac{C_{m_i} - \alpha_{m_i}}{\phi_{i+1} - d_{m_i}}, \frac{1 - y_j f(\boldsymbol{x}_j)}{\psi_j} \right\}_+, \tag{20}
$$

where ϕ_i denotes the i-th element of $\boldsymbol{\phi}$ and $d_i = C_i^{(\text{new})} - C_i^{(\text{old})}$. We used $\min_i\{z_i\}_+$ as a simplified notation of $\min_i\{z_i \mid z_i \geq 0\}$. Based on this largest possible $\Delta\theta$, we can compute $\boldsymbol{\alpha}$ and b along the solution path by (16).

At the border of the critical region, we need to update the index sets $\mathcal{M}$, $\mathcal{O}$, and $\mathcal{I}$. For example, if α_i $(i \in \mathcal{M})$ reaches 0, we need to move the element i from $\mathcal{M}$ to $\mathcal{O}$. Then the above path-following procedure is carried out again for the next critical region specified by the updated index sets $\mathcal{M}$, $\mathcal{O}$, and $\mathcal{I}$, and this procedure is repeated until $\boldsymbol{c}$ reaches $\boldsymbol{c}^{(\text{new})}$.

9

3.3 Empty Margin

In the above derivation, we have implicitly assumed that the index set $\mathcal{M}$ is not empty—when $\mathcal{M}$ is empty, we can not use (16) because $\boldsymbol{M}^{-1}$ does not exist.

When $\mathcal{M}$ is empty, the KKT conditions (6) can be re-written as

$$\sum_{j\in\mathcal{I}} Q_{ij}C_j + y_i b \geq 1, \qquad i \in \mathcal{O}, \tag{21a}$$

$$\sum_{j\in\mathcal{I}} Q_{ij}C_j + y_i b \leq 1, \qquad i \in \mathcal{I}, \tag{21b}$$

$$\sum_{i\in\mathcal{I}} y_i C_i = 0. \tag{21c}$$

Although we can not determine the value of b uniquely only from the above conditions, (21a) and (21b) specify the range of optimal b:

$$\max_{i\in\mathcal{L}} y_i g_i \leq b \leq \min_{i\in\mathcal{U}} y_i g_i, \tag{22}$$

where

$$g_i = 1 - \sum_{j\in\mathcal{I}} Q_{ij}C_j,$$

$$\mathcal{L} = \{i \mid i \in \mathcal{O}, y_i = 1\} \cup \{i \mid i \in \mathcal{I}, y_i = -1\},$$

$$\mathcal{U} = \{i \mid i \in \mathcal{O}, y_i = -1\} \cup \{i \mid i \in \mathcal{I}, y_i = 1\}.$$

Let

$$\delta \equiv \sum_{i\in\mathcal{I}} y_i d_i,$$

where

$$d_i = C_i^{(\text{new})} - C_i^{(\text{old})}.$$

When $\delta = 0$, the step size $\Delta\theta$ can be increased as long as the inequality (22) is satisfied. Violation of (22) can be checked by monitoring the upper and lower bounds of the bias b (which are piecewise-linear w.r.t. $\Delta\theta$) when $\Delta\theta$ is increased

$$\begin{aligned} u(\Delta\theta) &= \max_{i\in\mathcal{U}} y_i(g_i + \Delta g_i(\Delta\theta)), \\ \ell(\Delta\theta) &= \min_{i\in\mathcal{L}} y_i(g_i + \Delta g_i(\Delta\theta)), \end{aligned} \tag{23}$$

where

$$\Delta g_i(\Delta\theta) = -\Delta\theta \sum_{j\in\mathcal{I}} Q_{ij}d_j.$$

On the other hand, when $\delta \neq 0$, $\Delta\theta$ can not be increased without violating the equality condition (21c). In this case, an instance with index

$$i_{\text{low}} = \operatorname*{argmax}_{i\in\mathcal{L}} y_i g_i$$

10

or

$$i_{\mathrm{up}} = \operatorname*{argmin}_{i \in \mathcal{U}} y_i g_i$$

actually enters the index set $\mathcal{M}$. If the instance (we denote its index by m) comes from the index set $\mathcal{O}$, the following equation must be satisfied for keeping (21c) satisfied:

$$\Delta\theta\delta = -\Delta\alpha_m y_m.$$

Since $\Delta\theta > 0$ and $\Delta\alpha_m > 0$, we have

$$\operatorname{sign}(\delta) = \operatorname{sign}(-y_m).$$

On the other hand, if the instance comes from the index set $\mathcal{I}$,

$$\Delta\theta\delta = y_m(\Delta C_m - \Delta\alpha_m)$$

must be satisfied. Since $\Delta\theta > 0$ and $\Delta C_m - \Delta\alpha_m > 0$, we have

$$\operatorname{sign}(\delta) = \operatorname{sign}(y_m).$$

Considering these conditions, we arrive at the following updating rules for b and $\mathcal{M}$:

$$
\begin{array}{lll}
\delta > 0 & \Rightarrow & b = y_{i_{\mathrm{up}}} g_{i_{\mathrm{up}}}, \ \mathcal{M} = \{i_{\mathrm{up}}\}, \\
\delta < 0 & \Rightarrow & b = y_{i_{\mathrm{low}}} g_{i_{\mathrm{low}}}, \ \mathcal{M} = \{i_{\mathrm{low}}\}.
\end{array}
\tag{24}
$$

Note that we also need to remove i_{up} and i_{low} from $\mathcal{O}$ and $\mathcal{I}$, respectively.

3.4 Computational Complexity

The entire pseudo-code of the proposed WSVM path-following algorithm is described in Figure 3.

The computational complexity at each iteration of our path-following algorithm is the same as that for the ordinary SVM (i.e., the single-C formulation) (Hastie et al., 2004). Thus, our algorithm inherits a superior computational property of the original path-following algorithm.

The update of the linear system (17) from the previous one at each event point can be carried out efficiently with $O(|\mathcal{M}|^2)$ computational cost based on the *Cholesky decomposition rank-one update* (Golub and Van Loan, 1996) or the *block-matrix inversion formula* (Schott, 2005). Thus, the computational cost required for identifying the next event point is $O(n|\mathcal{M}|)$.

It is difficult to state the number of iterations needed for complete path-following because the number of events depends on the sensitivity of the model and the data set. Several empirical results suggest that the number of events linearly increases w.r.t. the data set size (Hastie et al., 2004; Gunter and Zhu, 2007; Wang et al., 2008); our experimental analysis given in Section 4 also showed the same tendency. This implies that path-following is computationally highly efficient—indeed, in Section 4, we will experimentally demonstrate that the proposed path-following algorithm is faster than an alternative approach in one or two orders of magnitude.

1: **arguments:**
2:     Optimal parameters $\boldsymbol{\alpha}$ and b for $\boldsymbol{c}^{(\mathrm{old})}$
3:     Sets $\mathcal{M}$, $\mathcal{O}$, $\mathcal{I}$, and Cholesky factor $\boldsymbol{L}$ of $\boldsymbol{Q}_{\mathcal{M}}$
4:     New weight vector $\boldsymbol{c}^{(\mathrm{new})}$
5: **end arguments**

6: **function** WSVM-PATH$(\boldsymbol{\alpha}, b, \boldsymbol{c}^{(\mathrm{old})}, \mathcal{M}, \mathcal{O}, \mathcal{I}, \boldsymbol{L}, \boldsymbol{c}^{(\mathrm{new})})$
7:     $\theta \leftarrow 0$, $\boldsymbol{c} \leftarrow \boldsymbol{c}^{(\mathrm{old})}$
8:     **while** $\theta \neq 1$ **do**
9:         **if** $\mathcal{M}$ is empty **then**
10:            $\Delta\theta \leftarrow$ EMPTYMARGIN
11:        **else**
12:            Calculate $\boldsymbol{\phi}$ by (17) using Cholesky factor $\boldsymbol{L}$
13:            Calculate $\boldsymbol{\psi}$ by (19)
14:            Calculate $\Delta\theta$ by (20)
15:        **end if**
16:        If $\theta + \Delta\theta > 1$, then $\Delta\theta \leftarrow 1 - \theta$
17:        Update $\boldsymbol{\alpha}$, b, and $\boldsymbol{c}$ by step length $\Delta\theta$
18:        $\theta \leftarrow \theta + \Delta\theta$
19:        Update $\mathcal{M}$, $\mathcal{O}$, and $\mathcal{I}$ depending on the event type
20:        Update $\boldsymbol{L}$ (Cholesky factor rank-one update)
21:    **end while**
22: **end function**

23: **function** EMPTYMARGIN
24:    **if** $\delta(\boldsymbol{\alpha}) \neq 0$ **then**
25:        Set bias term b by (24)
26:        $\Delta\theta \leftarrow 0$
27:    **else**
28:        Trace $u(\Delta\theta)$ and $\ell(\Delta\theta)$ in (23) until $u(\Delta\theta) = \ell(\Delta\theta)$
29:    **end if**
30:    **return** $\Delta\theta$
31: **end function**

Figure 3: Pseudo-code of the proposed WSVM path-following algorithm.

4. Experiments

In this section, we illustrate the empirical performance of the proposed WSVM path-following algorithm in a toy example and two real-world applications. We compared the computational cost of the proposed path-following algorithm with the *sequential minimal optimization* (SMO) algorithm (Platt, 1999) when the instance weights of WSVM are changed in various ways. In particular, we investigated the CPU time of updating solutions from some $\boldsymbol{c}^{(\mathrm{old})}$ to $\boldsymbol{c}^{(\mathrm{new})}$.

In the path-following algorithm, we assume that the optimal parameter $\boldsymbol{\alpha}$ as well as the Cholesky factor $\boldsymbol{L}$ of $\boldsymbol{Q}_{\mathcal{M}}$ for $\boldsymbol{c}^{(\text{old})}$ has already been obtained. In the SMO algorithm, we used the old optimal parameter $\boldsymbol{\alpha}$ as the initial starting point (i.e., the 'hot' start) after making them *feasible* using the *alpha-seeding strategy* (DeCoste and Wagstaff, 2000). We set the tolerance parameter in the termination criterion of SMO to 10^{-3}. Our implementation of the SMO algorithm is based on *LIBSVM* (Chang and Lin, 2001). To circumvent possible numerical instability, we added small positive constant 10^{-6} to the diagonals of the matrix $\boldsymbol{Q}$. In all the experiments, we used the Gaussian kernel

$$K(\boldsymbol{x}, \boldsymbol{x}') = \exp\left(-\frac{\gamma}{p}\|\boldsymbol{x} - \boldsymbol{x}'\|^2\right), \tag{25}$$

where γ is a hyper-parameter and p is the dimensionality of $\boldsymbol{x}$.

4.1 Illustrative Example

First, we illustrate the behavior of the proposed path-following algorithm using an artificial data set. Consider a binary classification problem with the training set $\{(\boldsymbol{x}_i, y_i)\}_{i=1}^n$, where $\boldsymbol{x}_i \in \mathbb{R}^2$ and $y_i \in \{-1, +1\}$. Let us define the sets of indices of positive and negative instances as $\mathcal{K}_{-1} = \{i|y_i = -1\}$ and $\mathcal{K}_{+1} = \{i|y_i = +1\}$, respectively. We assume that the loss function is defined as

$$\sum_i v_i I(y_i f(\boldsymbol{x}_i) \le 0), \tag{26}$$

where $v_i \in \{1, 2\}$ is the cost of misclassifying the instance $(\boldsymbol{x}_i, y_i)$, and $I(\cdot)$ is the indicator function. Let $\mathcal{D}_1 = \{i|v_i = 1\}$ and $\mathcal{D}_2 = \{i|v_i = 2\}$, i.e., $\mathcal{D}_2$ is the set of instance indices which have stronger influence on the overall test error than $\mathcal{D}_1$.

To be consistent with the above error metric, it would be natural to assign a smaller weight C_1 for $i \in \mathcal{D}_1$ and a larger weight C_2 for $i \in \mathcal{D}_2$ when training SVM. However, naively setting $C_2 = 2C_1$ is not generally optimal because the hinge loss is used in SVM training, while the 0-1 loss is used in performance evaluation (see (26)). In the following experiments, we fixed the Gaussian kernel width to $\gamma = 1$ and the instance weight for $\mathcal{D}_2$ to $C_2 = 10$, and we changed the instance weight C_1 for $\mathcal{D}_1$ from 0 to 10. Thus, the change of the weights is represented as

$$\begin{bmatrix} \boldsymbol{c}_{\mathcal{D}_1}^{(\text{old})} \\ \boldsymbol{c}_{\mathcal{D}_2}^{(\text{old})} \end{bmatrix} = \begin{bmatrix} \boldsymbol{0} \\ \boldsymbol{10} \end{bmatrix} \text{ and } \begin{bmatrix} \boldsymbol{c}_{\mathcal{D}_1}^{(\text{new})} \\ \boldsymbol{c}_{\mathcal{D}_2}^{(\text{new})} \end{bmatrix} = \begin{bmatrix} \boldsymbol{10} \\ \boldsymbol{10} \end{bmatrix}.$$

The two-dimensional input $\{\boldsymbol{x}_i\}_{i=1}^n$ were generated from the following distribution:

$$
\boldsymbol{x}_i \sim \begin{cases}
\mathcal{N}\left(\begin{bmatrix} 1 \\ 0 \end{bmatrix}, \begin{bmatrix} 1 & 0 \\ 0 & 0.5 \end{bmatrix}\right) & \text{if } i \in \mathcal{K}_{+1} \cap \mathcal{D}_1, \\[1em]
\mathcal{N}\left(\begin{bmatrix} 0 \\ 0 \end{bmatrix}, \begin{bmatrix} 0.5 & 0 \\ 0 & 0.5 \end{bmatrix}\right) & \text{if } i \in \mathcal{K}_{+1} \cap \mathcal{D}_2, \\[1em]
\mathcal{N}\left(\begin{bmatrix} 0 \\ 1 \end{bmatrix}, \begin{bmatrix} 1 & 0 \\ 0 & 0.5 \end{bmatrix}\right) & \text{if } i \in \mathcal{K}_{-1} \cap \mathcal{D}_1, \\[1em]
\mathcal{N}\left(\begin{bmatrix} 1 \\ 1 \end{bmatrix}, \begin{bmatrix} 0.5 & 0 \\ 0 & 0.5 \end{bmatrix}\right) & \text{if } i \in \mathcal{K}_{-1} \cap \mathcal{D}_2.
\end{cases} \tag{27}
$$

Figure 4 shows the generated instances for $n = 400$, in which instances in the above four cases have the equal size $n/4$. Before feeding the generated instances into algorithms, we normalized the inputs in $[0, 1]^2$.

Figure 5 shows piecewise-linear paths of some of the solutions α_i for $C_1 \in [0, 10]$ when $n = 400$. The left graph includes the solution paths of three representative parameters α_i for $i \in \mathcal{D}_1$. All three parameters increase as C_1 grows from zero, and one of the parameters (denoted by the dash-dotted line) suddenly drops down to zero at around $C_1 = 7$. Another parameter (denoted by the solid line) also sharply drops down at around $C_1 = 9$, and the last one (denoted by the dashed line) remains equal to C_1 until C_1 reaches 10. The right graph includes the solution paths of three representative parameters α_i for $i \in \mathcal{D}_2$, showing that their behavior is substantially different from that for $\mathcal{D}_1$. One of the parameters (denoted by the dash-dotted line) fluctuates significantly, while the other two parameters (denoted by the solid and dashed lines) are more stable and tend to increase as C_1 grows.

An important advantage of the path following algorithm is that the path of the validation error can be traced as well (see Figure 6). First, note that the path of the validation error (26) has piecewise-constant form because the 0-1 loss changes only when the sign of $f(\boldsymbol{x})$ changes. In our path-following algorithm, the path of $f(\boldsymbol{x})$ also has piecewise-linear form because $f(\boldsymbol{x})$ is linear in their parameters $\boldsymbol{\alpha}$ and b. Exploiting the piecewise linearity of $f(\boldsymbol{x})$, we can exactly detect the point at which the sign of $f(\boldsymbol{x})$ changes. These points correspond to the breakpoints of the piecewise-constant validation-error path. Figure 6 illustrates the relationship between the piecewise-linear path of $f(\boldsymbol{x})$ and the piecewise-constant validation-error path. Figure 7 shows an example of piecewise-constant validation-error path when C_1 is increased from 0 to 10, indicating that the lowest validation error was achieved at around $C_1 = 4$.

Finally, we investigated the computation time when the solution path from $C_1 = 0$ to 10 was computed. For comparison, we also investigated the computation time of the SMO algorithm when the solutions at every breakpoint were computed. We considered the following four cases: the number of training instances was $n = 400, 800, 1200,$ and 1600. For each n, we generated 10 data sets and the average and standard deviation over 10 runs are reported. Table 1 describes the results, showing that our path-following algorithm is faster than the SMO algorithm in one or two orders of magnitude; the difference between the two methods becomes more significant as the training data size n grows.

Data points in $\mathcal{D}_1$ Data points in $\mathcal{D}_2$ Data points in $\mathcal{D}_1 \cup \mathcal{D}_2$
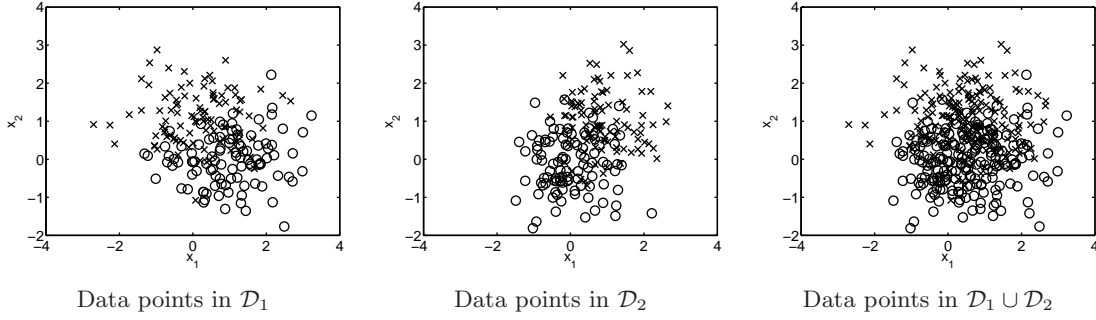
Figure 4: Artificial data set generated by the distribution (27). The crosses and circles indicate the data points in $\mathcal{K}_{-1}$ (negative class) and $\mathcal{K}_{+1}$ (positive class), respectively. The left plot shows the data points in $\mathcal{D}_1$ (misclassification cost is 1), the middle plot shows the data points in $\mathcal{D}_2$ (misclassification cost is 2), and the right plots show their union.

α_i for $i \in \mathcal{D}_1$ α_i for $i \in \mathcal{D}_2$

Figure 5: Examples of piecewise-linear paths of α_i for the artificial data set. The weights are changed from $C_i = 0$ to 10 for $i \in \mathcal{D}_1$ (for $i \in \mathcal{D}_2$, $C_i = 10$ is unchanged). The left and right plots show the paths of three representative parameters α_i for $i \in \mathcal{D}_1$, and for $i \in \mathcal{D}_2$, respectively.

The table also includes the number of events and the average number of elements in the margin set $\mathcal{M}$ (see Eq.(7b)). This shows that the number of events increases almost linearly in the sample size n, which well agrees with the empirical results reported in Hastie et al. (2004), Gunter and Zhu (2007), and Wang et al. (2008). The average number of elements in the set $\mathcal{M}$ increases very mildly as the sample size n grows.

4.2 Online Time-series Learning

In online time-series learning, larger (resp. smaller) weights should be assigned to newer (resp. older) instances. For example, in Cao and Tay (2003), the following weight function
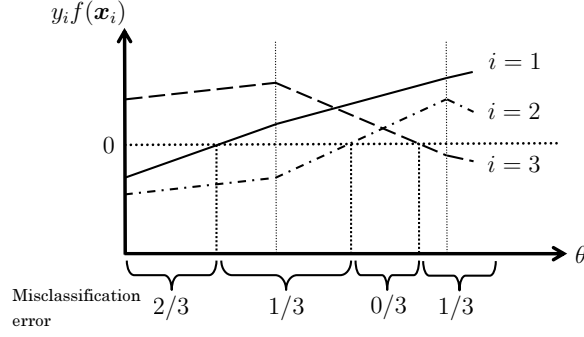
15

Figure 6: A schematic illustration of validation-error path. In this plot, the path of misclassification error rate $\frac{1}{3}\sum_{i=1}^{n} I(y_i f(\boldsymbol{x}_i)) \leq 0)$ for the 3 validation instances (x_1, y_1), (x_2, y_2), and (x_3, y_3) are depicted. The horizontal axis indicates the parameter θ and the vertical axis denotes $y_i f(\boldsymbol{x}_i)$, $i = 1, 2, 3$. The path of the validation error has piecewise-constant form because the 0-1 loss changes only when $f(\boldsymbol{x}_i) = 0$. The breakpoints of the piecewise-constant validation-error path can be exactly detected by exploiting the piecewise linearity of $f(\boldsymbol{x}_i)$.

Figure 7: An example of the validation-error path for 1000 validation instances of the artificial data set. The number of training instances is 400 and the Gaussian kernel with $\gamma = 1$ is used.

Table 1: The experimental results of the artificial data set. The average and the standard deviation (in brackets) over 10 runs are reported.

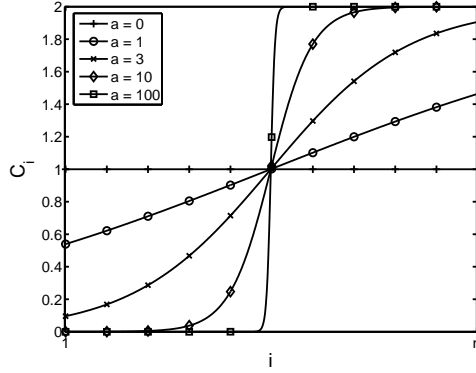| n	CPU time (sec.)		#events	mean $|\mathcal{M}|$
	path	SMO		
400	0.03 (0.00)	0.39 (0.01)	326.70 (7.17)	3.07 (0.03)
800	0.08 (0.00)	2.84 (0.12)	635.30 (17.47)	3.27 (0.02)
1200	0.19 (0.00)	10.63 (0.38)	997.60 (26.85)	3.38 (0.05)
1600	0.35 (0.01)	28.11 (0.77)	1424.00 (31.27)	3.50 (0.02)

16

Figure 8: The weight functions for financial time-series forecasting (Cao and Tay, 2003). The horizontal axis is the index of training instances which is sorted according to time (the most recent instance is $i = n$). If we set $a = 0$, all the instances are weighted equally.
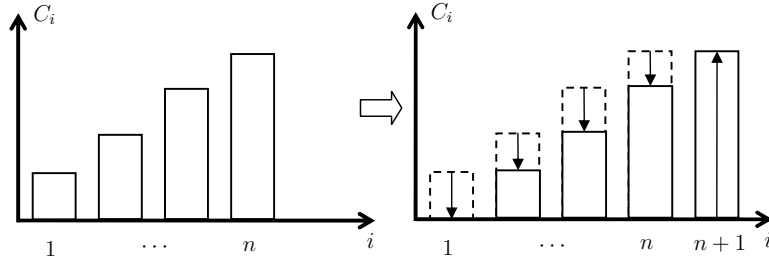

Figure 9: A schematic illustration of the change of weights in time-series learning. The left plot shows the fact that larger weights are assigned to more recent instances. The right plot describes a situation where we receive a new instance $(i = n + 1)$. In this situation, the oldest instance $(i = 1)$ is deleted by setting its weight to zero, the weight of the new instance is set to be the largest, and the weights of the rest of the instances are decreased accordingly.

is used:

$$C_i = C_0 \frac{2}{1 + \exp(a - 2a \times \frac{i}{n})}, \tag{28}$$

where C_0 and a are hyper-parameters and the instances are assumed to be sorted along the time axis (the most recent instance is $i = n$). Figure 8 shows the profile of the weight function (28) when $C_0 = 1$. In online learning, we need to update parameters when new observations arrive, and all the weights must be updated accordingly (see Figure 9).

We investigated the computational cost of updating parameters when several new observations arrive. The experimental data are obtained from the *NASDAQ composite index* between January 2, 2001 and December 31, 2009. As Cao and Tay (2003) and Chen et al.

Table 2: Features for financial forecasting ($p(i)$ is the closing price of the ith day and $\text{EMA}_k(i)$ is the k-day exponential moving average of the ith day.

Feature	Formula
EMA15	$p(i) - \text{EMA}_{15}(i)$
RDP-5	$(p(i) - p(i-5))/p(i-5) * 100$
RDP-10	$(p(i) - p(i-10))/p(i-10) * 100$
RDP-15	$(p(i) - p(i-15))/p(i-15) * 100$
RDP-20	$(p(i) - p(i-20))/p(i-20) * 100$
RDP+5	$\overline{(p(i+5) - p(i))}/p(i) * 100$
	$\overline{p(i)} = \text{EMA}_3(i)$

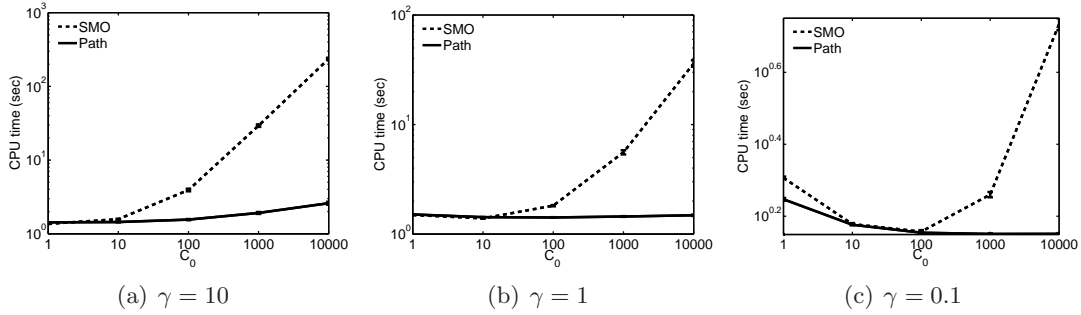(a) $\gamma = 10$ (b) $\gamma = 1$ (c) $\gamma = 0.1$

Figure 10: CPU time comparison for online time-series learning using NASDAQ composite index.

(2006), we transformed the original closing prices using the Relative Difference in Percentage (RDP) of the price and the exponential moving average (EMA).

Extracted features are listed in Table 2 (see Cao and Tay, 2003, for more details). Our task is to predict the sign of RDP+5 using EMA15 and four lagged-RDP values (RDP-5, RDP-10, RDP-15, and RDP-20). RDP values which exceed ± 2 standard deviations are replaced with the closest marginal values. We have an initial set of training instances with size $n = 2515$. The inputs were normalized in $[0, 1]^p$, where p is the dimensionality of the input $\boldsymbol{x}$. We used the Gaussian kernel (25) with $\gamma \in \{10, 1, 0.1\}$, and the weight parameter a in (28) was set to 3. We first trained WSVM using the initial set of instances. Then we added 5 instances to the previously trained WSVM and removed the oldest 5 instances by decreasing their weights to 0. This does not change the size of the training data set, but the entire weights need to be updated as illustrated in Figure 9. We iterated this process 5 times and compared the total computational costs of the path-following algorithm and the SMO algorithm. For fair comparison, we cleared the cache of kernel values at each update before running the algorithms.

Figure 10 shows the average CPU time over 10 runs for $C_0 \in \{1, 10, 10^2, 10^3, 10^4\}$, showing that the path-following algorithm is much faster than the SMO algorithm especially for large C_0.

4.3 Model Selection in Covariate Shift Adaptation

Covariate shift is a situation in supervised learning where the input distributions change between the training and test phases but the conditional distribution of outputs given inputs remains unchanged (Shimodaira, 2000). Under covariate shift, standard SVM and SVR are biased, and the bias caused by covariate shift can be asymptotically canceled by weighting the loss function according to the *importance* (i.e., the ratio of training and test input densities).

Here, we apply importance-weighted SVMs to *brain-computer interfaces* (BCIs) (Dornhege et al., 2007). A BCI is a system which allows for a direct communication from man to machine via brain signals. Strong non-stationarity effects have been often observed in brain signals between training and test sessions, which could be modeled as covariate shift (Sugiyama et al., 2007). We used the BCI datasets provided by the Berlin BCI group (Burde and Blankertz, 2006), containing 24 binary classification tasks. The input features are 4-dimensional preprocessed *electroencephalogram* (EEG) signals, and the output labels correspond to the 'left' and 'right' commands. The size of training datasets is around 500 to 1000, and the size of test datasets is around 200 to 300.

Although the importance-weighted SVM tends to have lower bias, it in turns has larger estimation variance than the ordinary SVM (Shimodaira, 2000). Thus, in practice, it is desirable to slightly 'flatten' the instance weights so that the trade-off between bias and variance is optimally controlled. Here, we changed the instance weights from the uniform values to the importance values using the proposed path-following algorithm, i.e., the instance weights were changed from $C_i^{(\text{old})} = C_0$ to $C_i^{(\text{new})} = C_0 \frac{p_{test}(\boldsymbol{x}_i)}{p_{train}(\boldsymbol{x}_i)}$, $i = 1, \ldots, n$. The importance values $\frac{p_{test}(\boldsymbol{x}_i)}{p_{train}(\boldsymbol{x}_i)}$ were estimated by the method proposed in Kanamori et al. (2009), which directly estimates the density ratio without going through density estimation of $p_{test}(\boldsymbol{x})$ and $p_{train}(\boldsymbol{x})$.

For comparison, we ran the SMO algorithm at (i) each breakpoint of the solution path, and (ii) 100 weight vectors taken uniformly in $[C_i^{(\text{old})}, C_i^{(\text{new})}]$. We used the Gaussian kernel and the inputs were normalized in $[0, 1]^p$, where p is the dimensionality of $\boldsymbol{x}$.

Figure 11 shows the average CPU time and its standard deviation. We examined several settings of hyper-parameters $\gamma \in \{10, 1, \ldots, 10^{-2}\}$ and $C_0 \in \{1, 10, 10^2, \ldots, 10^4\}$. The horizontal axis of each plot represents C_0. The graphs show that our path-following algorithm is faster than the SMO algorithm in all cases. While the SMO algorithm tended to take longer time for large C_0, the CPU time of the path-following algorithm did not increase with respect to C_0.

5. Beyond Classification

So far, we focused on classification scenarios. Here we show that the proposed path-following algorithm can be extended to various scenarios including regression, ranking, and transduction.
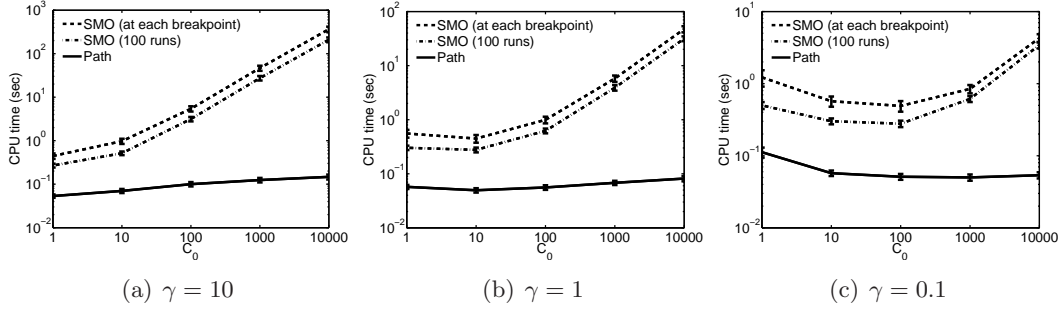
(a) $\gamma = 10$ (b) $\gamma = 1$ (c) $\gamma = 0.1$

Figure 11: CPU time comparison for covariate shift adaptation using BCI data.

5.1 Regression

The *support vector regression* (SVR) is a variant of SVM for regression problems (Vapnik et al., 1996; Mattera and Haykin, 1999; Müller et al., 1999).

5.1.1 FORMULATION

The primal optimization problem for the weighted SVR (WSVR) is defined by

$$
\min_{\boldsymbol{w},b,\{\xi_i,\xi_i^*\}_{i=1}^n} \quad \frac{1}{2}\|\boldsymbol{w}\|_2^2 + \sum_{i=1}^n C_i(\xi_i + \xi_i^*),
$$
$$
\text{s.t.} \quad y_i - f(\boldsymbol{x}_i) \leq \varepsilon + \xi_i,
$$
$$
f(\boldsymbol{x}_i) - y_i \leq \varepsilon + \xi_i^*,
$$
$$
\xi_i, \xi_i^* \geq 0, \ i = 1, \ldots, n,
$$

where $\epsilon > 0$ is an insensitive-zone thickness. Note that, as in the classification case, WSVR is reduced to the original SVR when $C_i = C$ for $i = 1, \ldots, n$. Thus, WSVR includes SVR as a special case.

The corresponding dual problem is given by

$$
\max_{\{\alpha_i\}_{i=1}^n} \quad -\frac{1}{2}\sum_{i=1}^n\sum_{j=1}^n \alpha_i\alpha_j K(\boldsymbol{x}_i,\boldsymbol{x}_j) - \varepsilon\sum_{i=1}^n |\alpha_i| + \sum_{i=1}^n y_i\alpha_i
$$
$$
\text{s.t.} \quad \sum_{i=1}^n \alpha_i = 0, \ -C_i \leq \alpha_i \leq C_i, \ i = 1, \ldots, n.
$$

The final solution, i.e., the regression function $f : \mathcal{X} \to \mathbb{R}$, is in the following form:

$$
f(\boldsymbol{x}) = \sum_{i=1}^n \alpha_i K(\boldsymbol{x},\boldsymbol{x}_i) + b.
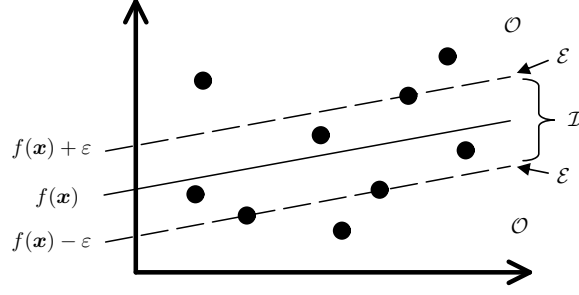$$

Figure 12: Partitioning of data points in SVR.

The KKT conditions for the above dual problem are given as

$$|y_i - f(\boldsymbol{x}_i)| \leq \varepsilon, \quad \text{if} \quad \alpha_i = 0, \tag{29a}$$

$$|y_i - f(\boldsymbol{x}_i)| = \varepsilon, \quad \text{if} \quad 0 < |\alpha_i| < C_i, \tag{29b}$$

$$|y_i - f(\boldsymbol{x}_i)| \geq \varepsilon, \quad \text{if} \quad |\alpha_i| = C_i, \tag{29c}$$

$$\sum_{i=1}^{n} \alpha_i = 0. \tag{29d}$$

Then the training instances can be partitioned into the following three index sets (see Figure 12):

$$\mathcal{O} = \{i : |y_i - f(\boldsymbol{x}_i)| \geq \varepsilon, |\alpha_i| = C_i\},$$
$$\mathcal{E} = \{i : |y_i - f(\boldsymbol{x}_i)| = \varepsilon, 0 < |\alpha_i| < C_i\},$$
$$\mathcal{I} = \{i : |y_i - f(\boldsymbol{x}_i)| \leq \varepsilon, \alpha_i = 0\}.$$

Let

$$\boldsymbol{K}^{\mathcal{E}} = \begin{bmatrix} 0 & \boldsymbol{1}^{\top} \\ \boldsymbol{1} & \boldsymbol{K}_{\mathcal{E}} \end{bmatrix} \quad \text{and} \quad \boldsymbol{s} = \begin{bmatrix} \operatorname{sign}(y_1 - f(\boldsymbol{x}_1)) \\ \vdots \\ \operatorname{sign}(y_n - f(\boldsymbol{x}_n)) \end{bmatrix}.$$

Then, from (29), we obtain

$$\begin{bmatrix} b \\ \boldsymbol{\alpha}_{\mathcal{E}} \end{bmatrix} = -(\boldsymbol{K}^{\mathcal{E}})^{-1} \begin{bmatrix} \boldsymbol{1}_{\mathcal{O}}^{\top} \\ \boldsymbol{K}_{\mathcal{E},\mathcal{O}} \end{bmatrix} \boldsymbol{c}_{\mathcal{O}} + (\boldsymbol{K}^{\mathcal{E}})^{-1} \begin{bmatrix} 0 \\ \boldsymbol{y}_{\mathcal{E}} - \varepsilon \boldsymbol{s}_{\mathcal{E}} \end{bmatrix},$$
$$\boldsymbol{\alpha}_{\mathcal{O}} = \operatorname{diag}(\boldsymbol{s}_{\mathcal{O}}) \boldsymbol{c}_{\mathcal{O}},$$
$$\boldsymbol{\alpha}_{\mathcal{O}} = \boldsymbol{0}.$$

where $\operatorname{diag}(\boldsymbol{s}_{\mathcal{O}})$ indicates the diagonal matrix with its diagonal part $\boldsymbol{s}_{\mathcal{O}}$. These functions are *affine* w.r.t. $\boldsymbol{c}$, so we can easily detect an event point by monitoring the inequalities in (29). We can follow the solution path of SVR by using essentially the same technique as SVM classification (and thus the details are omitted).

21

5.1.2 EXPERIMENTS ON REGRESSION

As an application of WSVR, we consider a heteroscedastic regression problem, where output noise variance depends on input points. In heteroscedastic data modeling, larger (resp. smaller) weights are usually assigned to instances with smaller (resp. larger) variances. Since the point-wise variances are often unknown in practice, they should also be estimated from data. A standard approach is to alternately estimate the weight vector c based on the current WSVR solution and update the WSVR solutions based on the new weight vector c (Kersting et al., 2007).

We set the weights as

$$C_i = C_0 \frac{\widehat{\sigma}}{|e_i|}, \tag{30}$$

where $e_i = y_i - \widehat{f}(\boldsymbol{x}_i)$ is the residual of the instance $(\boldsymbol{x}_i, y_i)$ from the current fit $\widehat{f}(\boldsymbol{x}_i)$, and $\widehat{\sigma}$ is an estimate of the common standard deviation of the noise computed as $\widehat{\sigma} = \sqrt{\frac{1}{n} \sum_{i=1}^{n} e_i^2}$. We employed the following procedure for the heteroscedastic data modeling:

Step1: Training WSVR with uniform weights (i.e., $C_i = C_0, i = 1, \ldots, n.$).

Step2: Update weights by (30) and update the solution of WSVR accordingly. Repeat this step until $\frac{1}{n} \sum_{i=1}^{n} |(e_i^{(\text{old})} - e_i)/e_i^{(\text{old})}| \leq 10^{-3}$ holds, where $e^{(\text{old})}$ is the previous training error.

We investigated the computational cost of Step2. We applied the above procedure to the well-known *Boston housing* data set. The sample size is 506 and the number of features is $p = 13$. The inputs were normalized in $[-1, 1]^p$. We randomly sampled $n = 404$ instances from the original data set, and the experiments were repeated 10 times. We used the Gaussian kernel (25) with $\gamma \in \{10, 1, 0.1\}$. The insensitive zone thickness in WSVR was fixed to $\varepsilon = 0.05$.

Each plot of Figure 13 shows the CPU time comparison for $C_0 \in \{1, 10, \ldots, 10^4\}$, and Figure 14 shows the number of iterations performed in Step2. Our path-following approach is faster than the SMO algorithm especially for large C_0.

5.2 Ranking

Recently, the problem of *learning to rank* has attracted wide interest as a challenging topic in machine learning and information retrieval (Liu, 2009). Here, we focus on a method called the *ranking SVM* (RSVM) (Herbrich et al., 2000).

5.2.1 FORMULATION

Assume that we have a set of n triplets $\{(\boldsymbol{x}_i, y_i, q_i)\}_{i=1}^{n}$ where $\boldsymbol{x}_i \in \mathbb{R}^p$ is a feature vector of an item and $y_i \in \{r_1, \ldots, r_q\}$ is a relevance of $\boldsymbol{x}_i$ to a query q_i. The relevance has an order of the preference $r_q \succ r_{q-1} \succ \cdots \succ r_1$, where $r_q \succ r_{q-1}$ means that r_q is preferred to r_{q-1}. The goal is to learn a ranking function $f(\boldsymbol{x})$ which returns a larger value for a preferred item. More precisely, for items $\boldsymbol{x}_i$ and $\boldsymbol{x}_j$ such that $q_i = q_j$, we want the ranking function $f(\boldsymbol{x})$ to satisfy

$$y_i \succ y_j \quad \Leftrightarrow \quad f(\boldsymbol{x}_i) > f(\boldsymbol{x}_j).$$

(a) $\gamma = 10$ (b) $\gamma = 1$ (c) $\gamma = 0.1$

Figure 13: CPU time comparison for heteroscedastic modeling using Boston housing data.

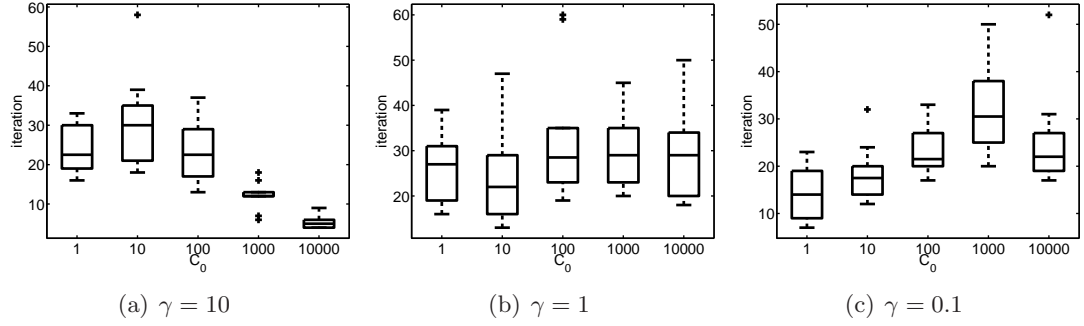(a) $\gamma = 10$ (b) $\gamma = 1$ (c) $\gamma = 0.1$

Figure 14: The number of weight updates for Boston housing data.

Let us define the following set of pairs:

$$\mathcal{P} = \{(i,j) \mid y_i \succ y_j, q_i = q_j\}.$$

RSVM solves the following optimization problem:

$$\min_{\boldsymbol{w}, \{\xi_{ij}\}_{(i,j) \in \mathcal{P}}} \quad \frac{1}{2} \|\boldsymbol{w}\|_2^2 + C \sum_{(i,j) \in \mathcal{P}} \xi_{ij}$$
$$\text{s.t.} \quad f(\boldsymbol{x}_i) - f(\boldsymbol{x}_j) \geq 1 - \xi_{ij}, \ (i,j) \in \mathcal{P}.$$

In practical ranking tasks such as information retrieval, a pair of items with highly different preference levels should have a larger weight than those with similar preference levels. Based on this prior knowledge, Cao et al. (2006) and Xu et al. (2006) proposed to assign different weights C_{ij} to different relevance pairs $(i,j) \in \mathcal{P}$. This is a *cost-sensitive* variant of RSVM whose primal problem is given as

$$\min_{\boldsymbol{w}, \{\xi_{ij}\}_{(i,j) \in \mathcal{P}}} \quad \frac{1}{2} \|\boldsymbol{w}\|_2^2 + \sum_{(i,j) \in \mathcal{P}} C_{ij} \xi_{ij}$$
$$\text{s.t.} \quad f(\boldsymbol{x}_i) - f(\boldsymbol{x}_j) \geq 1 - \xi_{ij}, \ (i,j) \in \mathcal{P}.$$

Since this formulation is interpreted as a WSVM for pairs of items $(i,j) \in \mathcal{P}$, we can easily apply our multi-parametric path approach. Note that the solution path algorithm for the

23

cost-sensitive RSVM is regarded as an extension of the previous work by Arreola et al. (2008), in which the solution path for the standard RSVM was studied.

In this paper, we consider a model selection problem for the weighting pattern $\{C_{ij}\}_{(i,j)\in\mathcal{P}}$. We assume that the weighting pattern is represented as

$$C_{ij} = C_{ij}^{(\mathrm{old})} + \theta(C_{ij}^{(\mathrm{new})} - C_{ij}^{(\mathrm{old})}), \ (i,j) \in \mathcal{P}, \ \theta \in [0,1], \tag{31}$$

where

$$C_{ij}^{(\mathrm{old})} = C_0, \ (i,j) \in \mathcal{P}, \tag{32}$$

$$C_{ij}^{(\mathrm{new})} = (2^{y_i} - 2^{y_j})C_0, \ (i,j) \in \mathcal{P}, \tag{33}$$

and C_0 is the common regularization parameter[2]. We follow the multi-parametric solution path from $\{C_{ij}^{(\mathrm{old})}\}_{(i,j)\in\mathcal{P}}$ to $\{C_{ij}^{(\mathrm{new})}\}_{(i,j)\in\mathcal{P}}$ and the best θ is selected based on the validation performance.

The performance of ranking algorithms is usually evaluated by some information-retrieval measures such as the *normalized discounted cumulative gain* (NDCG) (Järvelin and Kekäläinen, 2000). Consider a query q and define $q(j)$ as the index of the j-th largest item among $\{f(\boldsymbol{x}_i)\}_{i\in\{i|q_i=q\}}$. The NDCG at position k for a query q is defined as

$$\mathrm{NDCG@}k = Z \sum_{j=1}^{k} \left\{ \begin{array}{ll} 2^{y_{q(j)}} - 1, & j = 1, \\ \frac{2^{y_{q(j)}}-1}{\log(j)}, & j > 1, \end{array} \right. \tag{34}$$

where Z is a constant to normalize the NDCG in $[0,1]$. Note that the NDCG value in (34) is defined using only the top k items and the rest are ignored. The NDCG for multiple queries are defined as the average of (34).

The goal of our model selection problem is to choose θ with the largest NDCG value. As explained below, we can identify θ that attains the exact maximum NDCG value for validation samples by exploiting the piecewise linearity of the solution path. The NDCG value changes only when there is a change in the top k ranking, and the rank of two items $\boldsymbol{x}_i$ and $\boldsymbol{x}_j$ changes only when $f(\boldsymbol{x}_i)$ and $f(\boldsymbol{x}_j)$ cross. Then change points of the NDCG can be exactly identified because $f(\boldsymbol{x})$ changes in piecewise-linear form. Figure 15 schematically illustrates piecewise-linear paths and the corresponding NDCG path for validation samples. The validation NDCG changes in piecewise-constant form, and change points are found when there is a crossing between two piecewise-linear paths.

5.2.2 EXPERIMENTS ON RANKING

We used the OHSUMED data set from the LETOR package (version 3.0) provided by Microsoft Research Asia (Liu et al., 2007). We used the query-level normalized version of the data set containing 106 queries. The total number of query-document pairs is 16140,

---

2. In Chapelle and Keerthi (2010), ranking of each item is also incorporated to define the weighting pattern. However, these weights depend on the current ranking, and it might change during training. We thus, for simplicity, introduce the weighting pattern (33) that depends only on the difference of the preference levels.
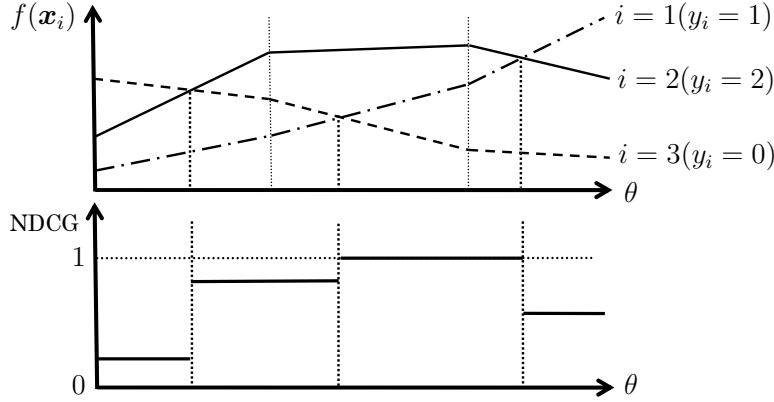
Figure 15: The schematic illustration of the NDCG path. The upper plot shows outputs for 3 items which have different levels of preferences y. The bottom plot shows the changes of the NDCG. Since the NDCG depends on the sorted order of items, it changes only when two lines of the upper plot intersect.

and the number of features is $p = 45$. The data set provided is originally partitioned into 5 subsets, each of which has training, validation, and test sets for 5-fold cross validation. Here, we only used the training and the validation sets.

We compared the CPU time of our path algorithm and the SMO algorithm to change $\{C_{ij}\}_{(i,j)\in\mathcal{P}}$ from flat ones (32) to relevance weighted ones (33). We need to modify the SMO algorithm to train the model without the explicit bias term b. The usual SMO algorithm updates selected two parameters per iteration to ensure that the solution satisfies the equality constraint derived from the optimality condition of b. Since RSVM has no bias term, the algorithm is adapted to update one parameter per iteration (Vogt, 2002). We employed the update rule of Vogt (2002) to adapt the SMO algorithm to RSVM and we chose the maximum violating point as an update parameter. This strategy is analogous to the maximum violating-pair working set selection of Keerthi et al. (2001) in ordinary SVM. Since it took relatively large computational time, we ran the SMO algorithm only at 10 points uniformly taken in $[C_{ij}^{(\mathrm{old})}, C_{ij}^{(\mathrm{new})}]$. We considered every pair of initial weight $C_0 \in \{10^{-5}, \ldots, 10^{-1}\}$ and Gaussian width $\gamma \in \{10, 1, 0.1\}$. The results, given in Figure 16, show that the path algorithm is faster than the SMO in all of the settings.

The CPU time of the path algorithm in Figure 16(a) increases as C_0 increases because the number of breakpoints and the size of the set $\mathcal{M}$ also increase. Since our path algorithm solves a linear system with size $|\mathcal{M}|$ using $O(|\mathcal{M}|^2)$ update in each iteration, practical computational time depends on $|\mathcal{M}|$ especially in large data sets. In the case of RSVM, the maximum value of $|\mathcal{M}|$ is the number of pairs of training documents $m = |\mathcal{P}|$. For each fold of the OHSUMED data set, $m = 367663, 422716, 378087, 295814$, and 283484. If $|\mathcal{M}| \approx m$, a large computational cost may be needed for updating the linear system. However, as Figure 17 shows, the size $|\mathcal{M}|$ is at most about one hundred in this setup.

Figure 18 shows the example of the path of validation NDCG@10. Since the NDCG depends on the sorted order of documents, direct optimization is rather difficult (Liu, 2009).
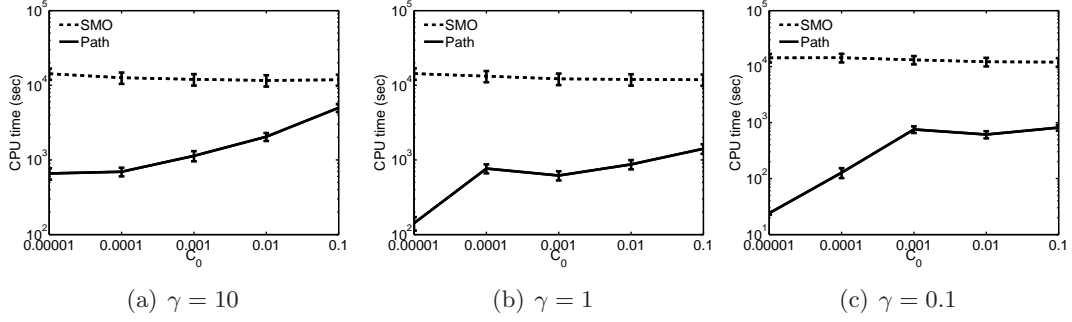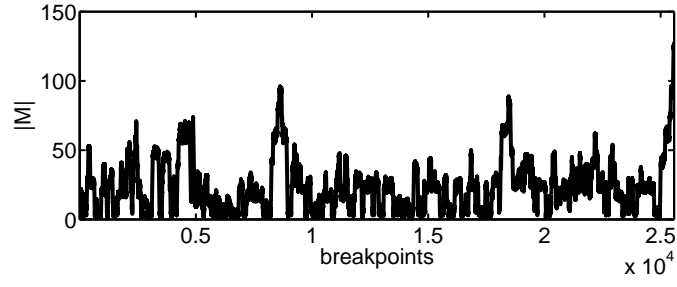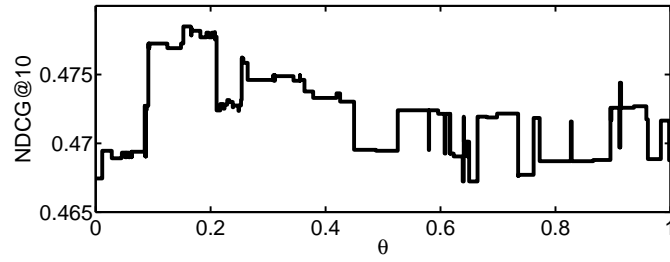
(a) $\gamma = 10$ (b) $\gamma = 1$ (c) $\gamma = 0.1$

Figure 16: CPU time comparison for RSVM.

Figure 17: The number of instances on the margin $|\mathcal{M}|$ in ranking experiment.

Figure 18: The change of NDCG@10 for $\gamma = 0.1$ and $C = 0.01$. The parameter θ in the horizontal axis is used as $\boldsymbol{c}^{(\mathrm{old})} + \theta(\boldsymbol{c}^{(\mathrm{new})} - \boldsymbol{c}^{(\mathrm{old})})$.

Using our path algorithm, however, we can detect the exact behavior of the NDCG by monitoring the change of scores $f(\boldsymbol{x})$ in the validation data set. Then we can find the best weighting pattern by choosing θ with the maximum NDCG for the validation set.

5.3 Transduction

In *transductive inference* (Vapnik, 1995), we are given unlabeled instances along with labeled instances. The goal of transductive inference is not to estimate the true decision function, but to classify the given unlabeled instances correctly. The *transductive SVM* (TSVM) (Joachims, 1999) is one of the most popular approaches to transductive binary classification. The objective of the TSVM is to maximize the classification margin for both labeled and unlabeled instances.

5.3.1 FORMULATION

Suppose we have k unlabeled instances $\{\boldsymbol{x}_i^*\}_{i=1}^k$ in addition to n labeled instances $\{(\boldsymbol{x}_i, y_i)\}_{i=1}^n$. The optimization problem of TSVM is formulated as

$$\min_{\{y_i^*, \xi_i^*\}_{i=1}^k, \boldsymbol{w}, b, \{\xi_i\}_{i=1}^n} \quad \frac{1}{2}\|\boldsymbol{w}\|_2^2 + C\sum_{i=1}^n \xi_i + C^*\sum_{j=1}^k \xi_j^* \tag{35}$$

$$\text{s.t.} \quad \begin{array}{ll} y_i(\boldsymbol{w}^\top \boldsymbol{\Phi}(\boldsymbol{x}_i) + b) \geq 1 - \xi_i, & i = 1, \ldots, n, \\ y_j^*(\boldsymbol{w}^\top \boldsymbol{\Phi}(\boldsymbol{x}_j) + b) \geq 1 - \xi_j^*, & j = 1, \ldots, k, \\ \xi_i \geq 0, & i = 1, \ldots, n, \\ \xi_j^* \geq 0, & j = 1, \ldots, k, \end{array}$$

where C and C^* are the regularization parameters for labeled and unlabeled data, respectively, and $y_j^* \in \{-1, +1\}, j = 1, \ldots, k$, are the labels of the unlabeled instances $\{\boldsymbol{x}_i^*\}_{i=1}^k$. Note that (35) is a combinatorial optimization problem with respect to $\{y_j^*\}_{j \in \{1,\ldots,k\}}$. The optimal solution of (35) can be found if we solve binary SVMs for all possible combinations of $\{y_j^*\}_{j \in \{1,\ldots,k\}}$, but this is computationally intractable even for moderate k. To cope with this problem, Joachims (1999) proposed an algorithm which approximately optimizes (35) by solving a series of WSVMs. The subproblem is formulated by assigning temporarily estimated labels $\widehat{y}_j^*$ to unlabeled instances:

$$\min_{\{\xi_i^*\}_{i=1}^k, \boldsymbol{w}, b, \{\xi_i\}_{i=1}^n} \quad \frac{1}{2}\|\boldsymbol{w}\|_2^2 + C\sum_{i=1}^n \xi_i + C_-^*\sum_{j \in \{j | \widehat{y}_j^* = -1\}} \xi_j^* + C_+^*\sum_{j \in \{j | \widehat{y}_j^* = 1\}} \xi_j^* \tag{36}$$

$$\text{s.t.} \quad \begin{array}{ll} y_i(\boldsymbol{w}^\top \boldsymbol{\Phi}(\boldsymbol{x}_i) + b) \geq 1 - \xi_i, & i = 1, \ldots, n, \\ \widehat{y}_j^*(\boldsymbol{w}^\top \boldsymbol{\Phi}(\boldsymbol{x}_j) + b) \geq 1 - \xi_j^*, & j = 1, \ldots, k, \\ \xi_i \geq 0, & i = 1, \ldots, n, \\ \xi_j^* \geq 0, & j = 1, \ldots, k, \end{array}$$

where C_-^* and C_+^* are the weights for unlabeled instances for $\{j \mid \widehat{y}_j^* = -1\}$ and $\{j \mid \widehat{y}_j^* = +1\}$, respectively. The entire algorithm is given as follows (see Joachims, 1999, for details):

Step1: Set the parameters C, C^*, and k^+, where k^+ is defined as

$$k^+ = k \times \frac{|\{j \mid y_j = +1, j = 1, \ldots, n\}|}{n}.$$

k^+ is defined so that the balance of positive and negative instances in the labeled set is equal to that in the unlabeled set.

Step2: Optimize the decision function using only the labeled instances and compute the decision function values $\{f(\boldsymbol{x}_j^*)\}_{j=1}^k$. Assign positive label $y_j^* = 1$ to the top k^+ unlabeled instances in decreasing order of $f(\boldsymbol{x}_j^*)$, and negative label $y_j^* = -1$ to the remaining instances. Set C_-^* and C_+^* to some small values (see Joachims, 1999, for details).

Step3: Train SVM using all the instances (i.e., solve (36)). Switch the labels of a pair of positive and negative unlabeled instances if the objective value (35) is reduced, where the pair of instances are selected based on $\{\xi_j^*\}_{j \in \{1,...,k\}}$ (see Joachims, 1999, for details). Iterate this step until no data pair decreases the objective value.

Step4: Set $C_-^* = \min(2C_-^*, C^*)$ and $C_+^* = \min(2C_+^*, C^*)$. If $C_-^* \geq C^*$ and $C_+^* \geq C^*$, terminate the algorithm. Otherwise return to Step3.

Our path-following algorithm can be applied to Step3 and Step4 for improving computational efficiency. Step3 can be carried out via path-following as follows:

Step3(a) Choose a pair of positive instance $\boldsymbol{x}_m^*$ and negative instance $\boldsymbol{x}_{m'}^*$.

Step3(b) After removing the positive instance $\boldsymbol{x}_m^*$ by decreasing its weight parameter C_m from C_+^* to 0, add the instance $\boldsymbol{x}_m^*$ as a negative one by increasing C_m from 0 to C_-^*.

Step3(c) After removing the negative instance $\boldsymbol{x}_{m'}^*$ by decreasing its weight parameter $C_{m'}$ from C_-^* to 0, add the instance $\boldsymbol{x}_{m'}^*$ as a positive one by increasing $C_{m'}$ from 0 to C_+^*.

Note that the steps 3(b) and 3(c) for switching the labels may be merged into a single step. Step4 also can be carried out by our path-following algorithm.

5.3.2 EXPERIMENTS ON TRANSDUCTION

We compare the computation time of the proposed path-following algorithm and the SMO algorithm for Step3 and Step4 of TSVM. We used the *spam* data set obtained from the *UCI machine learning repository* (Asuncion and Newman, 2007). The sample size is 4601, and the number of features is $p = 57$. We randomly selected 10% of data set as labeled instances, and the remaining 90% were used as unlabeled instances. The inputs were normalized in $[0,1]^p$.

Figure 19 shows the average CPU time and its standard deviation over 10 runs for the Gaussian width $\gamma \in \{10, 1, 0.1\}$ and $C \in \{1, 10, 10^2, \ldots, 10^4\}$. The figure shows that our algorithm is consistently faster than the SMO algorithm in all of these settings.

6. Discussion and Conclusion

In this paper, we developed an efficient algorithm for updating solutions of instance-weighted SVMs. Our algorithm was built upon multiple parametric programming techniques, and it is an extension of existing single-parameter path-following algorithms to multiple parameters.

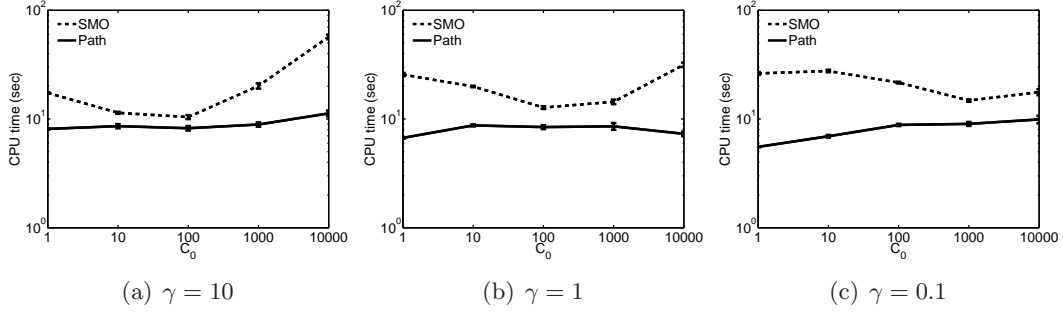(a) $\gamma = 10$ (b) $\gamma = 1$ (c) $\gamma = 0.1$

Figure 19: CPU time comparison for the transductive SVM.

We experimentally demonstrated the computational advantage of the proposed algorithm on a wide range of applications including on-line time-series analysis, heteroscedastic data modeling, covariate shift adaptation, ranking, and transduction.

Another important advantage of the proposed approach beyond computational efficiency is that the exact solution path is represented in piecewise linear form. In SVM (and its variants), the decision function $f(\boldsymbol{x})$ also has a piecewise linear form because $f(\boldsymbol{x})$ is linear in the parameters $\boldsymbol{\alpha}$ and b. It enables us to compute the entire path of the validation errors and to select the model with the minimum validation error. Let $\mathcal{V}$ be the validation set and the validation loss is defined as $\sum_{i \in \mathcal{V}} \ell(y_i, f(\boldsymbol{x}_i))$. Suppose that the current weight is expressed as $\boldsymbol{c} + \theta \boldsymbol{d}$ in a critical region $\mathcal{R}$ using a parameter $\theta \in \mathbb{R}$, and the output has the form $f(\boldsymbol{x}_i) = a_i \theta + b_i$ for some scalar constants a_i and b_i. Then the minimum validation error in the current critical region $\mathcal{R}$ can be identified by solving the following optimization problem:

$$\min_{\theta \in \mathbb{R}} \sum_{i \in \mathcal{V}} \ell(y_i, a_i \theta + b_i) \ \text{ s.t. } \boldsymbol{c} + \theta \boldsymbol{d} \in \mathcal{R}. \tag{37}$$

After following the entire solution-path, the best model can be selected among the candidates in the finite number of critical regions. In the case of 0-1 loss, i.e.,

$$\ell(y_i, f(\boldsymbol{x}_i)) = I\{y_i \text{sgn}(f(\boldsymbol{x}_i)) = -1\},$$

the problem (37) can be solved by monitoring all the points at which $f(\boldsymbol{x}_i) = 0$ (see Figure 6). Furthermore, if the validation error is measured by squared loss

$$\ell(y_i, f(\boldsymbol{x}_i)) = (y_i - f(\boldsymbol{x}_i))^2,$$

the problem (37) can be analytically solved in each critical region. As another interesting example, we described how to find the maximum validation NDCG in ranking problem (see Section 5.2). In the case of NDCG, the problem (37) can be solved by monitoring all the intersections of $f(\boldsymbol{x}_i)$ and $f(\boldsymbol{x}_j)$ such that $y_i \neq y_j$ (see Figure 15)[3].

Although we focused only on quadratic programming (QP) machines in this paper, similar algorithms can be developed for linear programming (LP) machines. It is well-known

---

3. In NDCG case, the "min" is replaced with "max" in the optimization problem (37).

in the parametric programming literature that the solution of LP and QP have piecewise linear form if a linear function of hyper-parameters appears in the constant term of the constraints and/or the linear part of the objective function (see Ritter, 1984; Best, 1982; Gal, 1995; Pistikopoulos et al., 2007, for more details). Indeed, the parametric LP technique (Gal, 1995) has already been applied to several machine learning problems (Zhu et al., 2004; Yao and Lee, 2007; Li and Zhu, 2008). One of our future works is to apply the multi-parametric approach to these LP machines.

In this paper, we studied the changes of instance-weights of various types of SVMs. There are many other situations in which a path of multiple hyper-parameters can be exploited. For instance, the application of the multi-parametric path approach to the following problems would be interesting future works:

- Different (functional) margin SVM:

$$
\min_{\boldsymbol{w}, b, \{\xi_i\}_{i=1}^n} \quad \frac{1}{2} \|\boldsymbol{w}\|_2^2 + C \sum_{i=1}^n \xi_i,
$$
$$
\text{s.t.} \ \ y_i f(\boldsymbol{x}_i) \geq \delta_i - \xi_i, \ \xi_i \geq 0, \ i = 1, \ldots, n,
$$

where $\delta_i \in \mathbb{R}$ is a margin rescaling parameter. Chapelle and Keerthi (2010) indicated that this type of parametrization can be used to give different costs to each pair of items in ranking SVM.

- SVR with different insensitive-zone thickness. Although usual SVR has the common insensitive-zone thickness ε for all instances, different thickness ε_i for every instance can be assigned:

$$
\min_{\boldsymbol{w}, b, \{\xi_i, \xi_i^*\}_{i=1}^n} \quad \frac{1}{2} \|\boldsymbol{w}\|_2^2 + C \sum_{i=1}^n (\xi_i + \xi_i^*),
$$
$$
\text{s.t.} \quad y_i - f(\boldsymbol{x}_i) \leq \varepsilon_i + \xi_i,
$$
$$
f(\boldsymbol{x}_i) - y_i \leq \varepsilon_i + \xi_i^*,
$$
$$
\xi_i, \xi_i^* \geq 0, \ i = 1, \ldots, n.
$$

In the case of common thickness, the optimal ε is known to be asymptotically proportional to the noise variance (Smola et al., 1998; Kwok and Tsang, 2003). In the case of heteroscedastic noise, it would be reasonable to set different ε_i, each of which is proportional to the variance of each (iteratively estimated) y_i.

- The weighted lasso. The lasso solves the following quadratic programming problem (Tibshirani, 1996):

$$
\min_{\boldsymbol{\beta}} \|\boldsymbol{y} - \sum_{j=1}^p \boldsymbol{x}_j \beta_j\|_2^2 + \lambda \sum_{j=1}^p |\beta_j|,
$$

where λ is the regularization parameter. A weighted version of the lasso has been considered in Zou (2006):

$$
\min_{\boldsymbol{\beta}} \|\boldsymbol{y} - \sum_{j=1}^p \boldsymbol{x}_j \beta_j\|_2^2 + \lambda \sum_{j=1}^p w_j |\beta_j|,
$$

30

where w_j is an individual weight parameters for each β_j. The weights are adaptively determined by $w_j = |\hat{\beta}_j|^{-\gamma}$, where $\hat{\beta}_j$ is an initial estimation of β_j and $\gamma > 0$ is a parameter. A similar weighted parameter-minimization problem has also been considered in Candes et al. (2008) in the context of signal reconstruction. They considered the following weighted ℓ_1-minimization problem[4]:

$$\min_{\boldsymbol{x} \in \mathbb{R}^n} \quad \sum_{i=1}^{p} w_i |x_i|$$
$$\text{s.t.} \quad \boldsymbol{y} = \boldsymbol{\Phi}\boldsymbol{x}.$$

where $\boldsymbol{y} \in \mathbb{R}^m$, $\boldsymbol{\Phi} \in \mathbb{R}^{m \times n}$, and $m < n$. The goal of this problem is to reconstruct a sparse signal $\boldsymbol{x}$ from the measurement vector $\boldsymbol{y}$ and sensing matrix $\boldsymbol{\Phi}$. The constraint linear equations have infinitely many solutions and the simplest explanation of $\boldsymbol{y}$ is desirable. To estimate better sparse representation, they proposed an iteratively re-weighting strategy for estimating w_i.

In order to apply the multi-parametric approach to these problems, we need to determine the search direction of the path in the multi-dimensional hyper-parameter space. In many situations search directions can be estimated from data.

Incremental-decremental SVM (Cauwenberghs and Poggio, 2001; Martin, 2002; Ma and Theiler, 2003; Laskov et al., 2006; Karasuyama and Takeuchi, 2009) exploits the piecewise linearity of the solutions. It updates SVM solutions efficiently when instances are added or removed from the training set. The incremental and decremental operations can be implemented using our instance-weight path approach. If we want to add an instance $(\boldsymbol{x}_i, y_i)$, we increase C_i from 0 to some specified value. Conversely, if we want to remove an instance $(\boldsymbol{x}_j, y_j)$, we decrease C_j to 0. The paths generated by these two approaches are different in general. The instance-weight path keeps the optimality of all the instances including currently adding and/or removing ones. On the other hand, the incremental-decremental algorithm does not satisfy the optimality of adding and/or removing ones until the algorithm terminates. When we need to guarantee the optimality at intermediate points on the path, our approach is more useful.

In the parametric programming approach, numerical instabilities sometimes cause computational difficulty. In practical implementation, we usually update several quantities such as $\boldsymbol{\alpha}$, b, $yf(\boldsymbol{x}_i)$, and $\boldsymbol{L}$ from the previous values without calculating them from scratch. However, the rounding error may be accumulated at every breakpoints. We can avoid such accumulation using the *refresh strategy*: re-calculating variables from scratch, for example, every 100 steps (note that, in this case, we need $O(n|\mathcal{M}|^2)$ computations in every 100 steps). Fortunately, such numerical instabilities rarely occurred in our experiments, and the accuracy of the KKT conditions of the solutions were kept high enough.

Another (but related) numerical difficulty arises when the matrix $\boldsymbol{M}$ in (17) is close to singular. Wang et al. (2008) pointed out that if the matrix is singular, the update is no longer unique. To the best of our knowledge, this degeneracy problem is not fully solved in path-following literature. Many heuristics are proposed to circumvent the problem, and we used one of them in the experiments: adding small positive constant to the diagonal elements

---

4. Note that $\boldsymbol{x}$ and $\boldsymbol{y}$ in the above equation have different meanings from other parts of this paper.

of kernel matrix. Other strategies are also discussed in Wu et al. (2008), Gärtner et al. (2009), and Ong et al. (2010).

Scalability of our algorithm depends on the size of $\mathcal{M}$ because a linear system with $|\mathcal{M}|$ unknowns must be solved at each breakpoint. Although we can update the Cholesky factor by $O(|\mathcal{M}|^2)$ cost from the previous one, iterative methods such as conjugate-gradients may be more efficient than the direct matrix update when $|\mathcal{M}|$ is fairly large. When $|\mathcal{M}|$ is small the parametric programming approach can be applied to relatively large data sets such as more than tens of thousands of instances (see, for example, the ranking experiments in Section 5.2).

References

A. Albert. *Regression and the Moore-Penrose Pseudoinverse*. Academic Press, New York and London, 1972.

E. L. Allgower and K. Georg. Continuation and path following. *Acta Numerica*, 2:1–64, 1993.

N. Aronszajn. Theory of reproducing kernels. *Transactions of the American Mathematical Society*, 68:337–404, 1950.

K. Z. Arreola, T. Gärtner, G. Gasso, and S. Canu. Regularization path for ranking SVM. In *ESANN 2008, 16th European Symposium on Artificial Neural Networks, Bruges, Belgium, April 23-25, 2008, Proceedings*, pages 415–420, 2008.

A. Asuncion and D. Newman. UCI machine learning repository. `http://www.ics.uci.edu/~mlearn/MLRepository.html`, 2007.

F. Bach, D. Heckerman, and E. Horvitz. Considering cost asymmetry in learning classifiers. *Journal of Machine Learning Research*, 7:1713–1741, 2006.

K. P. Bennett and E. J. Bredensteiner. A parametric optimization method for machine learning. *INFORMS Journal on Computing*, 9(3):311–318, 1997.

M. J. Best. An algorithm for the solution of the parametric quadratic programming problem. Technical Report 82-24, Faculty of Mathematics, University of Waterloo, 1982.

S. Bickel, J. Bogojeska, T. Lengauer, and T. Scheffer. Multi-task learning for HIV therapy screening. In A. McCallum and S. Roweis, editors, *Proceedings of 25th Annual International Conference on Machine Learning (ICML2008)*, pages 56–63, Jul. 5–9 2008.

B. E. Boser, I. M. Guyon, and V. N. Vapnik. A training algorithm for optimal margin classifiers. In D. Haussler, editor, *Proceedings of the Fifth Annual ACM Workshop on Computational Learning Theory*, pages 144–152. ACM Press, 1992.

S. Boyd and L. Vandenberghe. *Convex Optimization*. Cambridge University Press, Cambridge, UK, 2004.

W. Burde and B. Blankertz. Is the locus of control of reinforcement a predictor of brain-computer interface performance? In *Proceedings of the 3rd International Brain-Computer Interface Workshop and Training Course 2006*, Graz, Austria, 2006. Verlag der Technischen Universität.

E. Candes, M. Wakin, and S. Boyd. Enhancing sparsity by reweighted ℓ_1 minimization. *Journal of Fourier Analysis and Applications*, 14(5-6):877–905, 2008.

L. Cao and F. Tay. Support vector machine with adaptive parameters in financial time series forecasting. *IEEE Transactions on Neural Networks*, 14(6):1506–1518, 2003.

Y. Cao, J. Xu, T.-Y. Liu, H. Li, Y. Huang, and H.-W. Hon. Adapting ranking SVM to document retrieval. In *SIGIR '06: Proceedings of the 29th annual international ACM SIGIR conference on Research and development in information retrieval*, pages 186–193, New York, NY, USA, 2006. ACM. ISBN 1-59593-369-7.

G. Cauwenberghs and T. Poggio. Incremental and decremental support vector machine learning. In T. K. Leen, T. G. Dietterich, and V. Tresp, editors, *Advances in Neural Information Processing Systems*, volume 13, pages 409–415, Cambridge, Massachussetts, 2001. The MIT Press.

C.-C. Chang and C.-J. Lin. LIBSVM: a library for support vector machines, 2001. Software available at `http://www.csie.ntu.edu.tw/~cjlin/libsvm`.

O. Chapelle and S. Keerthi. Efficient algorithms for ranking with SVMs. *Information Retrieval*, 13(3):201–215, 2010.

W.-H. Chen, J.-Y. Shih, and S. Wu. Comparison of support-vector machines and back propagation neural networks in forecasting the six major Asian stock markets. *Int. J. Electron. Financ.*, 1(1):49–67, 2006. ISSN 1746-0069.

C. Cortes and V. Vapnik. Support-vector networks. *Machine Learning*, 20:273–297, 1995.

D. DeCoste and K. Wagstaff. Alpha seeding for support vector machines. In *Proceedings of the International Conference on Knowledge Discovery and Data Mining*, pages 345–359, 2000.

G. Dornhege, J. Millán, T. Hinterberger, D. McFarland, and K.-R. Müller, editors. *Toward Brain Computer Interfacing*. MIT Press, Cambridge, MA, USA, 2007.

S. Fine and K. Scheinberg. Incremental learning and selective sampling via parametric optimization framework for svm. In T. G. Dietterich, S. Becker, and Z. Ghahramani, editors, *Advances in Neural Information Processing Systems 14*, Cambridge, MA, 2002. MIT Press.

T. Gal. *Postoptimal Analysis, Parametric Programming, and Related Topics*. Walter de Gruyter, 1995.

T. Gal and J. Nedoma. Multiparametric Linear Programming. *MANAGEMENT SCIENCE*, 18(7):406–422, 1972.

B. Gärtner, J. Giesen, M. Jaggi, and T. Welsch. A combinatorial algorithm to compute regularization paths. *arXiv cs.LG.*, 2009.

G. H. Golub and C. F. Van Loan. *Matrix computations*. Johns Hopkins University Press, Baltimore, MD, USA, 1996. ISBN 0801854148.

L. Gunter and J. Zhu. Efficient computation and model selection for the support vector regression. *Neural Computation*, 19(6):1633–1655, 2007. ISSN 0899-7667.

T. Hastie, S. Rosset, R. Tibshirani, and J. Zhu. The entire regularization path for the support vector machine. *Journal of Machine Learning Research*, 5:1391–1415, 2004.

R. Herbrich, T. Graepel, and K. Obermayer. Large margin rank boundaries for ordinal regression. In A. Smola, P. Bartlett, B. Schölkopf, and D. Schuurmans, editors, *Advances in Large Margin Classifiers*, pages 115–132, Cambridge, MA, 2000. MIT Press.

K. Järvelin and J. Kekäläinen. IR evaluation methods for retrieving highly relevant documents. In *SIGIR '00: Proceedings of the 23rd annual international ACM SIGIR conference on Research and development in information retrieval*, pages 41–48, New York, NY, USA, 2000. ACM. ISBN 1-58113-226-3.

J. Jiang and C. Zhai. Instance weighting for domain adaptation in NLP. In *Proceedings of the 45th Annual Meeting of the Association for Computational Linguistics*, pages 264–271, 2007.

T. Joachims. Transductive inference for text classification using support vector machines. In *Proceedings of the 16th Annual International Conference on Machine Learning (ICML 1999)*, pages 200–209, San Francisco, CA, USA, 1999. Morgan Kaufmann Publishers Inc.

T. Kanamori, S. Hido, and M. Sugiyama. A least-squares approach to direct importance estimation. *Journal of Machine Learning Research*, 10:1391–1445, Jul. 2009.

M. Karasuyama and I. Takeuchi. Multiple incremental decremental learning of support vector machines. In Y. Bengio, D. Schuurmans, J. Lafferty, C. K. I. Williams, and A. Culotta, editors, *Advances in Neural Information Processing Systems 22*, pages 907–915, 2009.

S. Keerthi, S. Shevade, C. Bhattacharyya, and K. Murthy. Improvements to platt's smo algorithm for svm classifier design. *Neural Computation*, 13(3):637–649, 2001.

K. Kersting, C. Plagemann, P. Pfaff, and W. Burgard. Most likely heteroscedastic Gaussian process regression. In Z. Ghahramani, editor, *Proceedings of the 24th Annual International Conference on Machine Learning (ICML 2007)*, pages 393–400. Omnipress, 2007.

J. Kwok and I. Tsang. Linear dependency between ε and the input noise in ε-support vector regression. *IEEE Transactions on Neural Networks*, 14(3):544–553, 2003.

P. Laskov, C. Gehl, S. Kruger, and K.-R. Müller. Incremental support vector learning: Analysis, implementation and applications. *Journal of Machine Learning Research*, 7:1909–1936, 2006.

G. Lee and C. Scott. The one class support vector machine solution path. In *ICASSP, IEEE International Conference on Acoustics, Speech and Signal Processing - Proceedings*, volume 2, pages II521–II524, 2007.

Y. Li and J. Zhu. l_1-norm quantile regression. *Journal of Computational and Graphical Statistics*, 17(1):163–185, 2008.

C.-F. Lin and S.-D. Wang. Fuzzy support vector machines. *IEEE Transactions on Neural Networks*, 13(2):464–471, 2002.

Y. Lin, Y. Lee, and G. Wahba. Support vector machines for classification in nonstandard situations. *Machine Learning*, 46(1/3):191–202, 2002.

T.-Y. Liu. Learning to rank for information retrieval. *Foundations and Trends in Information Retrieval*, 3(3):225–331, 2009.

T. Y. Liu, J. Xu, T. Qin, W. Xiong, and H. Li. LETOR: Benchmark dataset for research on learning to rank for information retrieval. In *SIGIR '07: Proceedings of the Learning to Rank workshop in the 30th annual international ACM SIGIR conference on Research and development in information retrieval*, 2007.

J. Ma and J. Theiler. Accurate online support vector regression. *Neural Computation*, 15 (11):2683–2703, 2003.

M. Martin. On-line support vector machines for function approximation. Technical report, Software Department, University Politecnica de Catalunya, 2002.

D. Mattera and S. Haykin. Support vector machines for dynamic reconstruction of a chaotic system. In B. Scholkopf, C. J. Burges, and A. J. Smola, editors, *Advances in kernel methods: support vector learning*, pages 211–241. MIT Press, Cambridge, MA, USA, 1999. ISBN 0-262-19416-3.

K.-R. Müller, A. J. Smola, G. Rätsch, B. Schökopf, J. Kohlmorgen, and V. Vapnik. Using support vector machines for time series prediction. In *Advances in kernel methods: support vector learning*, pages 243–253. MIT Press, Cambridge, MA, USA, 1999. ISBN 0-262-19416-3.

N. Murata, M. Kawanabe, A. Ziehe, K.-R. Müller, and S. Amari. On-line learning in changing environments with applications in supervised and unsupervised learning. *Neural Networks*, 15(4-6):743–760, 2002.

C.-J. Ong, S. Shao, and J. Yang. An improved algorithm for the solution of the regularization path of support vector machine. *IEEE Transactions on Neural Networks*, 21(3):451–462, 2010.

E. N. Pistikopoulos, M. C. Georgiadis, and V. Dua. *Process Systems Engineering: Volume 1: Multi-Parametric Programming*. WILEY-VCH, 2007.

J. C. Platt. Fast training of support vector machines using sequential minimal optimization. In B. Schölkopf, C. J. C. Burges, and A. J. Smola, editors, *Advances in Kernel Methods — Support Vector Learning*, pages 185–208, Cambridge, MA, 1999. MIT Press.

R. Raina, A. Battle, H. Lee, B. Packer, and A. Ng. Self-taught learning: transfer learning from unlabeled data. In Z. Ghahramani, editor, *Proceedings of the 24th Annual International Conference on Machine Learning (ICML 2007)*, pages 759–766. Omnipress, 2007.

K. Ritter. On parametric linear and quadratic programming problems. In R. Cottle, M. L. Kelmanson, and B. Korte, editors, *Mathematical Programming: Proceedings of the International Congress on Mathematical Programming*, pages 307–335. Elsevier Science Publisher B.V., 1984.

S. Rosset. Bi-level path following for cross validated solution of kernel quantile regression. *Journal of Machine Learning Research*, 10:2473–2505, 2009.

S. Rosset and J. Zhu. Piecewise linear regularized solution paths. *Annals of Statistics*, 35: 1012–1030, 2007.

J. R. Schott. *Matrix Analysis For Statistics*. Wiley-Interscience, 2005.

H. Shimodaira. Improving predictive inference under covariate shift by weighting the log-likelihood function. *Journal of Statistical Planning and Inference*, 90(2):227–244, 2000.

K. Sjostrand, M. Hansen, H. Larsson, and R. Larsen. A path algorithm for the support vector domain description and its application to medical imaging. *Medical Image Analysis*, 11(5):417–428, 2007.

A. J. Smola, N. Murata, B. Schölkopf, and K.-R. Müller. Asymptotically optimal choice of ε-loss for support vector machines. In L. Niklasson, M. Bodén, and T. Ziemke, editors, *Proceedings of the International Conference on Artificial Neural Networks*, Perspectives in Neural Computing, pages 105–110, Berlin, 1998. Springer.

M. Sugiyama, M. Krauledat, and K.-R. Müller. Covariate shift adaptation by importance weighted cross validation. *Journal of Machine Learning Research*, 8:985–1005, May 2007.

I. Takeuchi, Q. V. Le, T. D. Sears, and A. J. Smola. Nonparametric quantile estimation. *Journal of Machine Learning Research*, 7:1231–1264, 2006.

I. Takeuchi, K. Nomura, and T. Kanamori. Nonparametric conditional density estimation using piecewise-linear solution path of kernel quantile regression. *Neural Comput.*, 21(2): 533–559, 2009. ISSN 0899-7667.

R. Tibshirani. Regression shrinkage and selection via the lasso. *Journal of the Royal Statistical Society, Series B*, 58(1):267–288, 1996.

V. Vapnik, S. E. Golowich, and A. Smola. Support vector method for function approximation, regression estimation, and signal processing. In M. Mozer, M. Jordan, and T. Petsche, editors, *Advances in Neural Information Processing Systems 9*, pages 281–287. MIT Press, 1996.

V. N. Vapnik. *The Nature of Statistical Learning Theory*. Springer-Verlag, Berlin, Germany, 1995.

M. Vogt. SMO algorithms for support vector machines without bias term. Technical report, Technische Universität Darmstadt, 2002.

G. Wang, D.-Y. Yeung, and F. H. Lochovsky. A new solution path algorithm in support vector regression. *IEEE Transactions on Neural Networks*, 19(10):1753–1767, 2008.

Z. Wu, A. Zhang, and C. Li. Trace solution paths for SVMs via parametric quadratic programming. In *KDD Workshop Report DMMT'08: data mining using matrices and tensors*, 2008.

J. Xu, Y. Cao, H. Li, and Y. Huang. Cost-sensitive learning of SVM for ranking. In J. Fürnkranz, T. Scheffer, and M. Spiliopoulou, editors, *Machine Learning: ECML 2006, 17th European Conference on Machine Learning, Berlin, Germany, September 18-22, 2006, Proceedings*, volume 4212, pages 833–840. Springer, 2006.

X. Yang, Q. Song, and Y. Wang. A weighted support vector machine for data classification. *International Journal of Pattern Recognition and Artificial Intelligence*, 21(5):961–976, 2007.

Y. Yao and Y. Lee. Another look at linear programming for feature selection via methods of regularization. Technical Report 800, Department of Statistics, The Ohio State University, 2007.

J. Zhu, S. Rosset, T. Hastie, and R. Tibshirani. 1-norm support vector machines. In S. Thrun, L. Saul, and B. Schölkopf, editors, *Advances in Neural Information Processing Systems 16*, Cambridge, MA, 2004. MIT Press.

H. Zou. The adaptive lasso and its oracle properties. *Journal of the American Statistical Association*, 101(476):1418–1429, 2006.